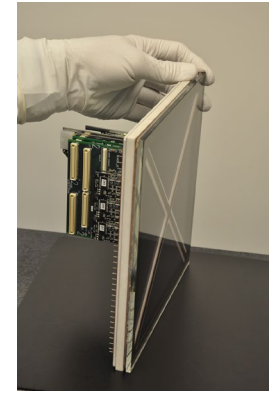
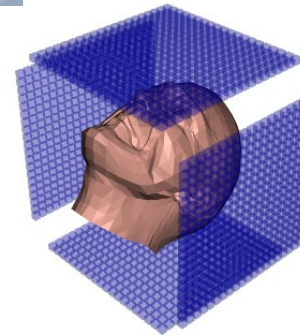
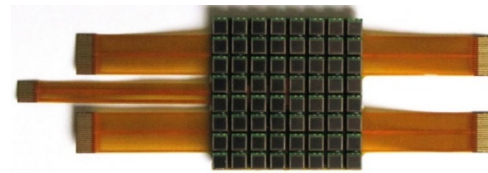
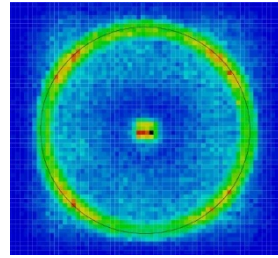
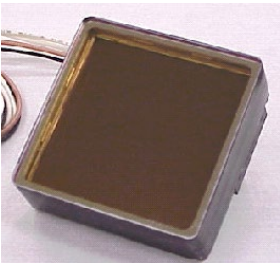


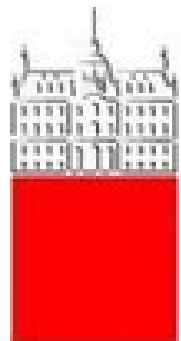


## 62<sup>nd</sup> International Winter Meeting on Nuclear Physics

19 - 23 January 2026  
Bormio, Italy

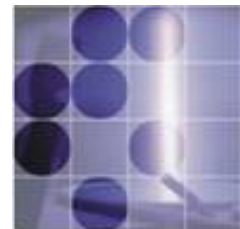


# Instrumentation for advances in PET medical imaging



Peter Križan

*University of Ljubljana and J. Stefan Institute*



# Interplay of detector R&D for particle/nuclear physics and medical imaging

---

Traditionally excellent collaboration of the two research areas.

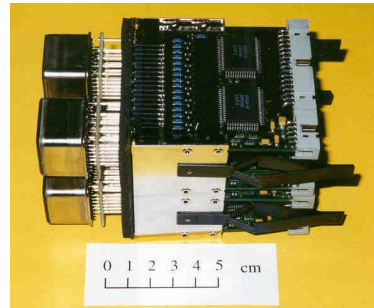
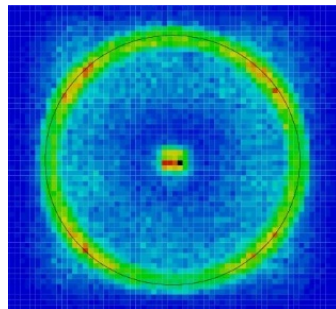
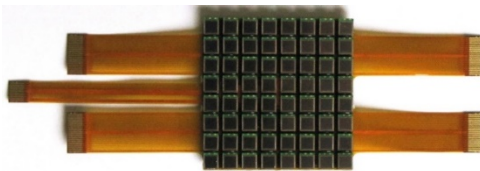
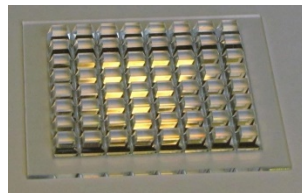
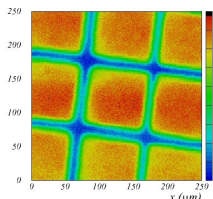
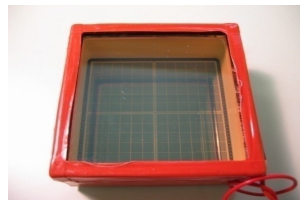
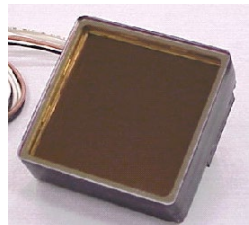
Novel detection techniques required in particle physics → with modifications, can often be applied in medical imaging  
... and sometimes also vice versa...

One of the recent examples: SiPMs as scintillation light sensors for

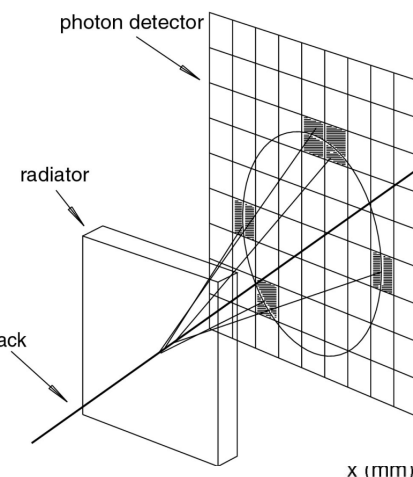
- Electromagnetic calorimeters, RICH counters, scintillating-fiber trackers
- Positron Emission Tomography (PET) scanners

Also: in HEP we are often small users, it helps us if a device becomes interesting for big users.

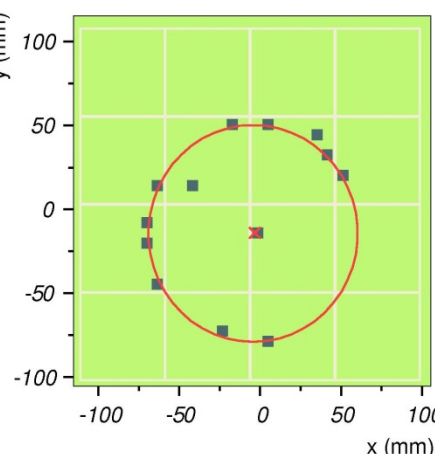
# Our original expertise in instrumentation: Cherenkov detectors, single-photon sensors and associated electronics



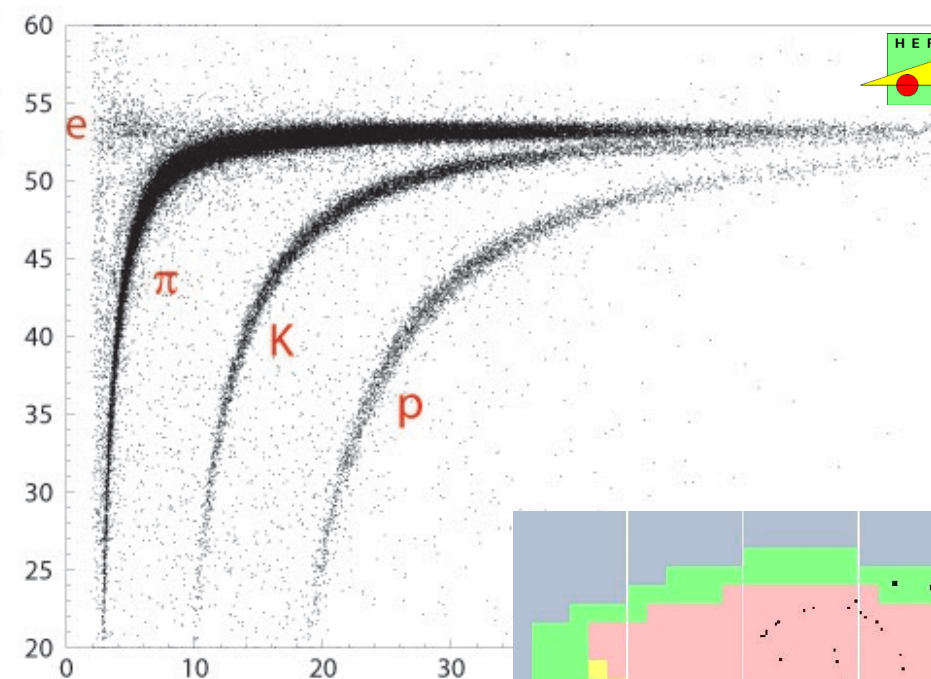
$v$  (mm)



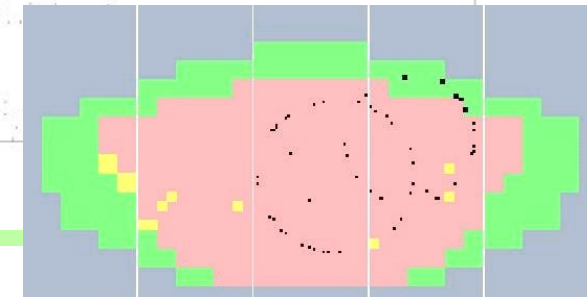
$y$  (mm)



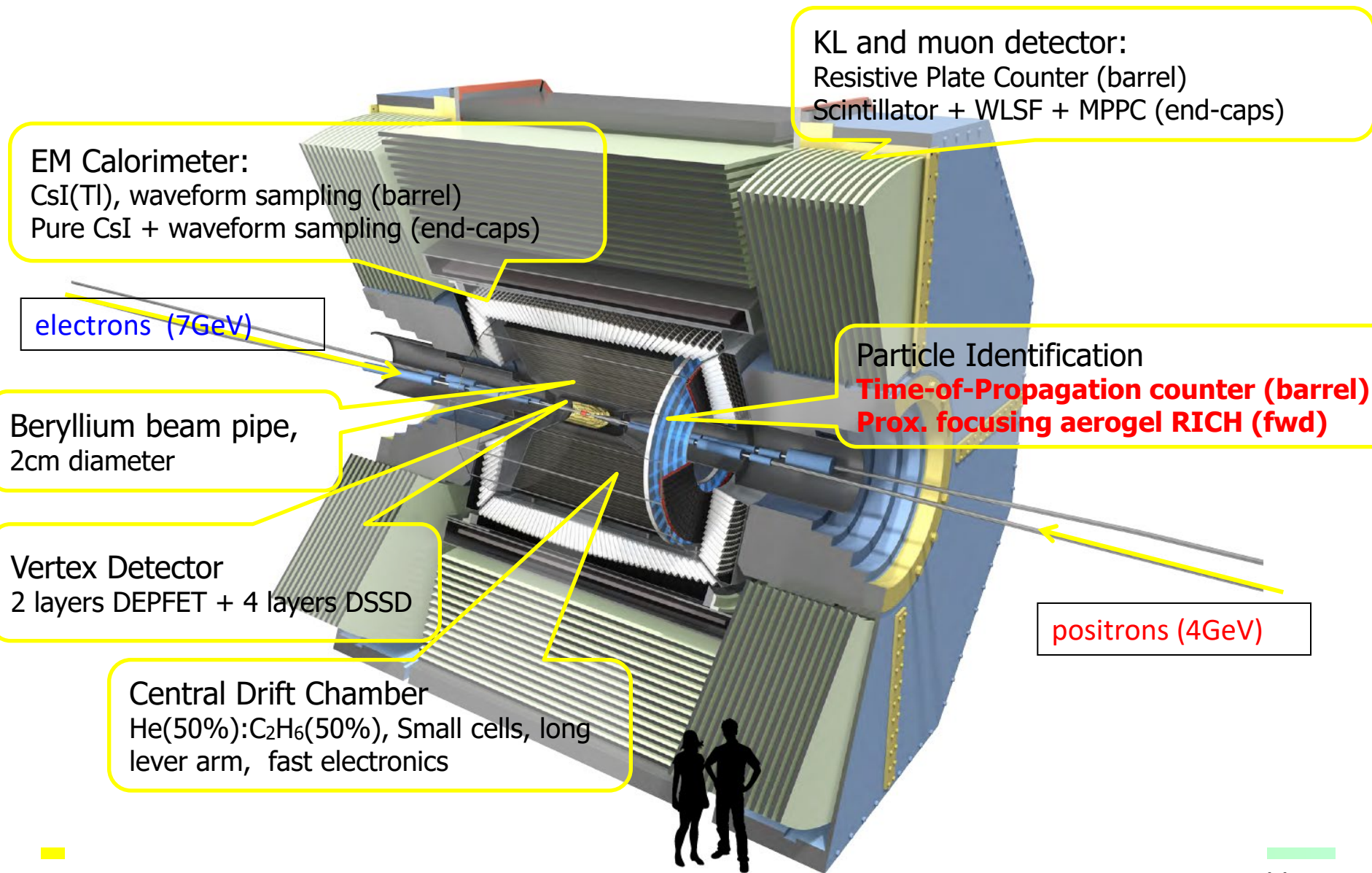
Cherenkov angle (mrad)



0 1 2 3 4 5 cm



# Belle II Detector



# Contents

---

PET – Positron Emission Tomography

Current topics in PET

Flexible limited angle PET scanner

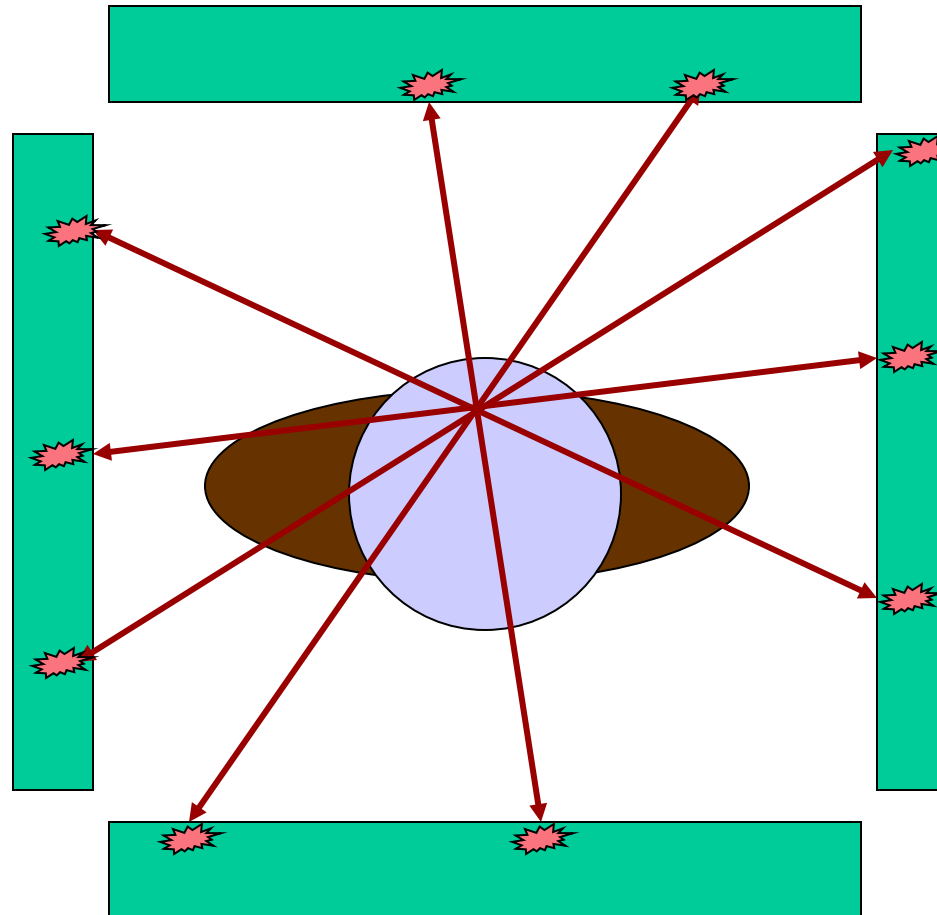
Cherenkov radiation-based PET scanner

Conclusions and summary

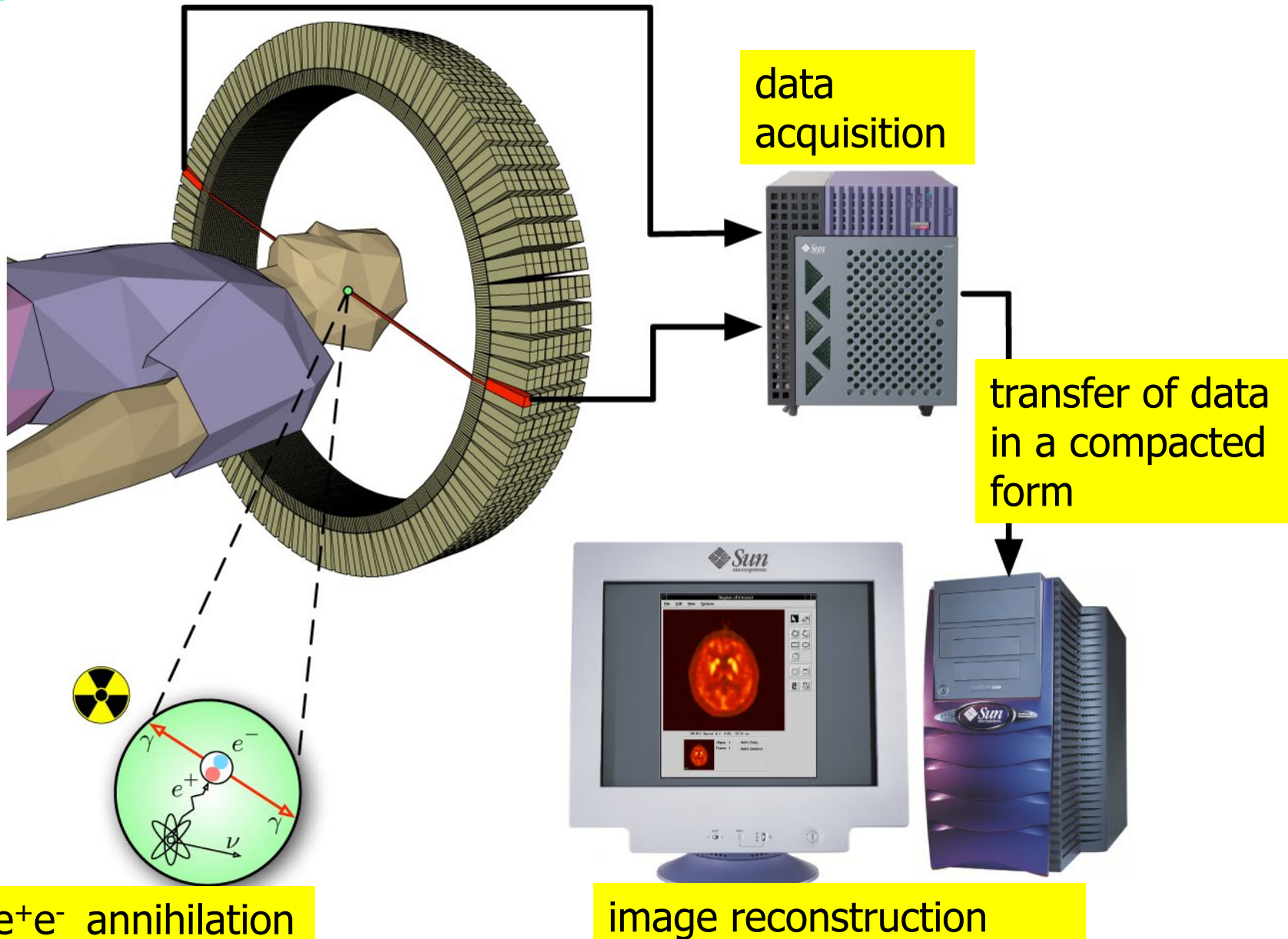
# PET: positron emission tomography

In the blood of the patient, a substance is administered that contains a radioactive isotope – a beta<sup>+</sup> emitter (e.g., fluorodeoxyglucose, FDG, with <sup>18</sup>F).

Positrons from the <sup>18</sup>F decay annihilate with electrons in the tissue, emitting a pair of collinear gammas.



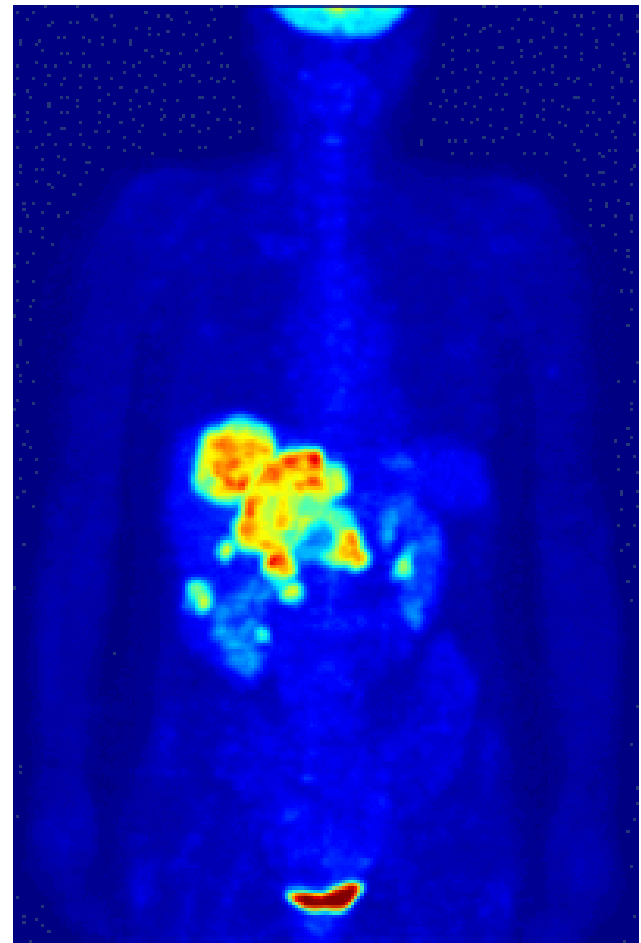
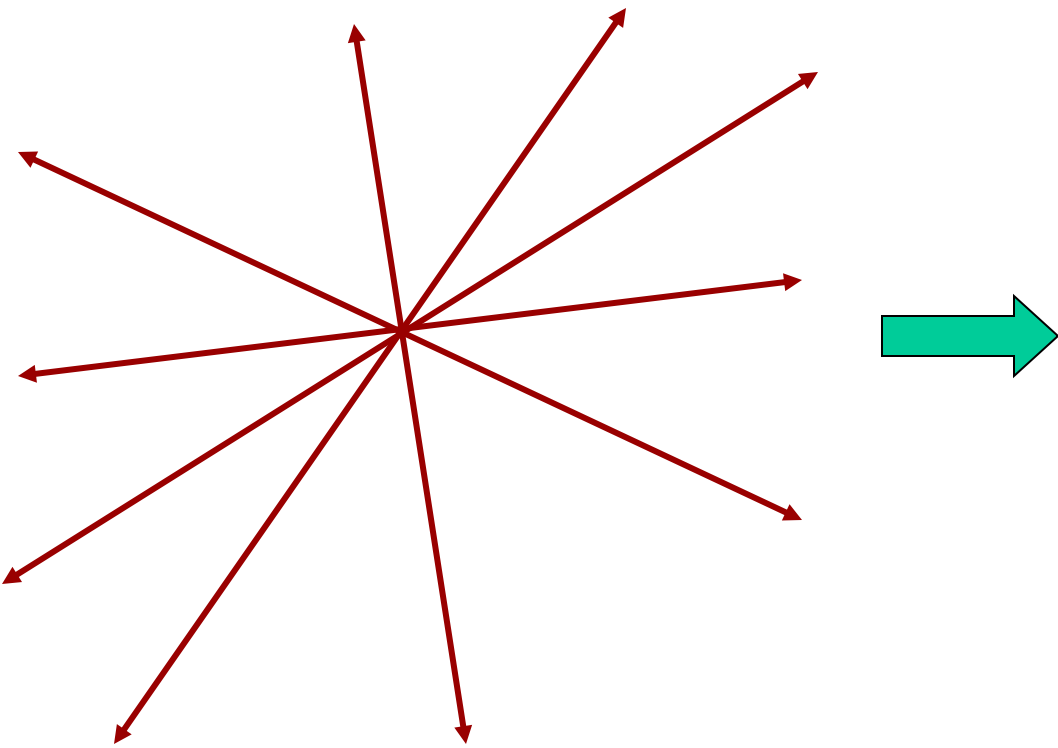
# PET: collection and handling of data



# PET: image reconstruction

Image reconstruction: from the position and direction of the lines determine the distribution of the radioactive fluorine in the body.

The places in the body with a higher substance concentration will show a higher activity.



# PET with a time-of-flight information

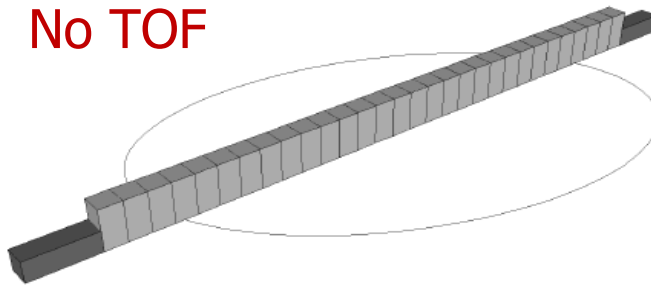
The emission point of the  $\gamma$  pair can be **anywhere on the line** between the two detector elements that have been hit.

Detectors can in principle also measure the **time of arrival** of each of the  $\gamma$  rays  
→ an **additional constraint** on the point of origin of the two  $\gamma$  rays along the line connecting the two detector hits  
→ **time-of-flight (TOF) PET**

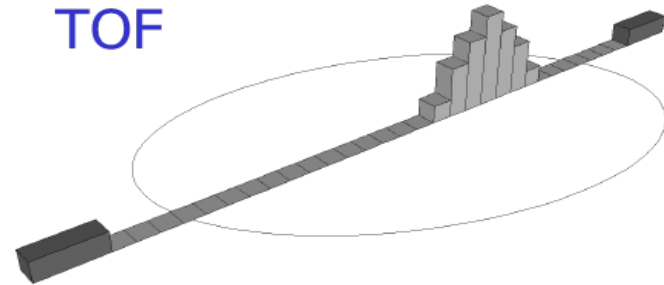
Good resolution in time-of-flight → **limits the number of hit pixels** along the line connecting the two detector hits

In the reconstruction step, each line contributes to fewer pixels  
→ **less noise** in the reconstructed image

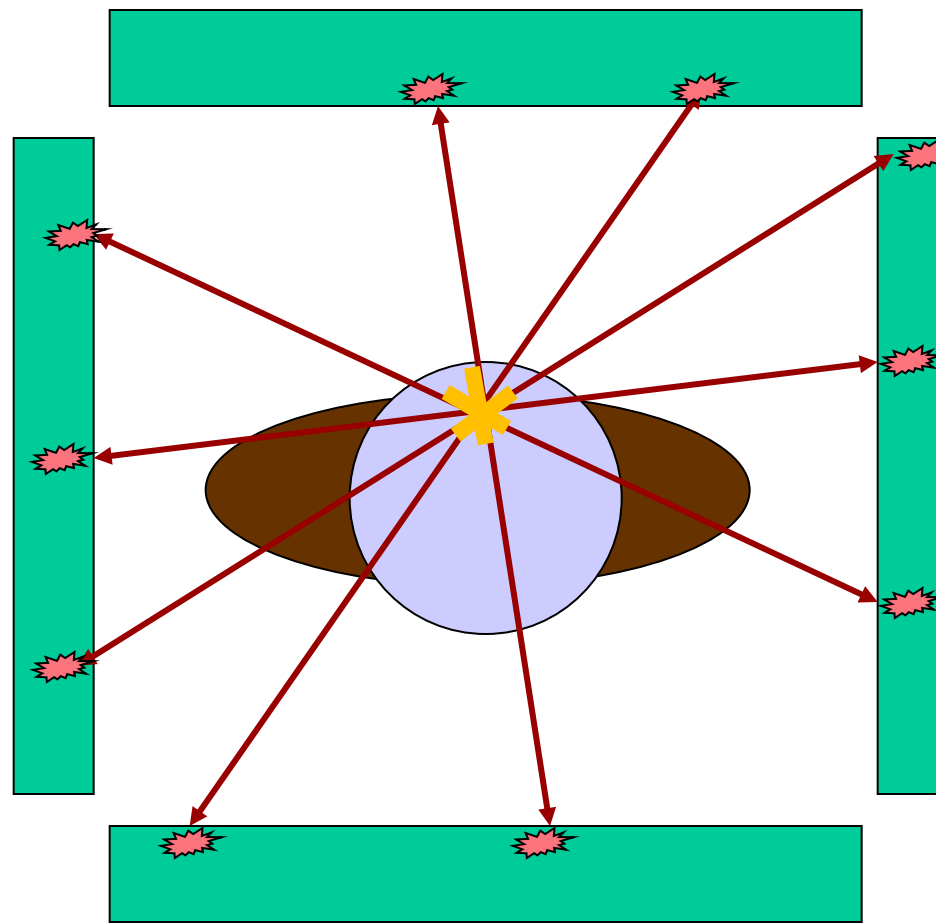
No TOF



TOF



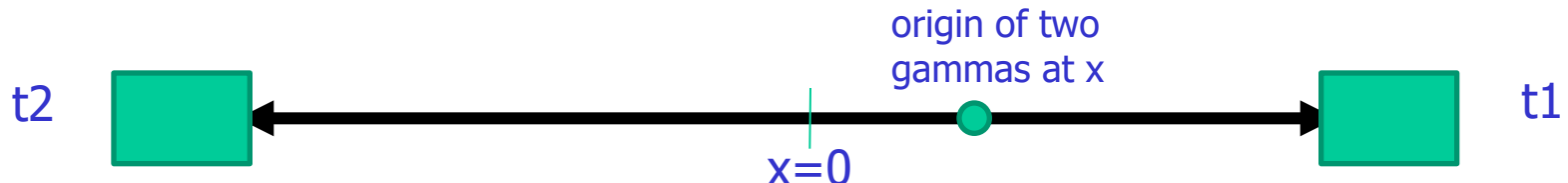
# TOF-PET: positron tomography with the time-of-arrival measurement



Good resolution in time-of-flight → limits the number of hit pixels along the line connecting the two detector hits  
In the reconstruction step, each line contributes to fewer pixels  
→ less noise in the reconstructed image

# TOF-PET: time resolution

What kind of time resolution is needed?



$$t_1 = (L/2 - x)/c \quad \text{source at } x, \text{ distance between detectors} = L$$

$$t_2 = (L/2 + x)/c$$

$$t_1 - t_2 = 2x/c \rightarrow x = (t_1 - t_2) c/2 \rightarrow \Delta x = \Delta(t_1 - t_2) c/2$$

resolution in TOF

$$\Delta(t_1 - t_2) = 300 \text{ ps} \rightarrow \Delta x = 4.5 \text{ cm}$$

$$\Delta(t_1 - t_2) = 66 \text{ ps} \rightarrow \Delta x = 1 \text{ cm}$$

$\Delta(t_1 - t_2)$  – CTR, coincidence timing resolution (FWHM)

Effective sensitivity  $S_{\text{eff},D} \propto \eta_{\text{det}}^2 \eta_{\text{geom}} \frac{D}{\Delta t}$

- $\eta_{\text{det}}$  - detection efficiency of the detector
- $\eta_{\text{geom}}$  - the geometrical efficiency (angular coverage)
- $D$  - diameter of the object imaged
- $\Delta t$  - coincidence timing resolution - CTR

Optimize detector CTR ( $\Delta t$ ) to maximize the sensitivity

# Motivation for Fast TOF PET

- Paradigm shift in medicine:
  - From the treatment of an obvious disease
  - To early diagnosis / prevention
- This leads to more stringent requirements on PET diagnostics
  - Sensitivity (=positive→positive)
  - Specificity (=negative→negative)
- Targeted Radionuclide Therapy (TRT) & Theranostics\*
  - introduced an urgent need for more widespread and accurate PET

Number of PET scanners per million people

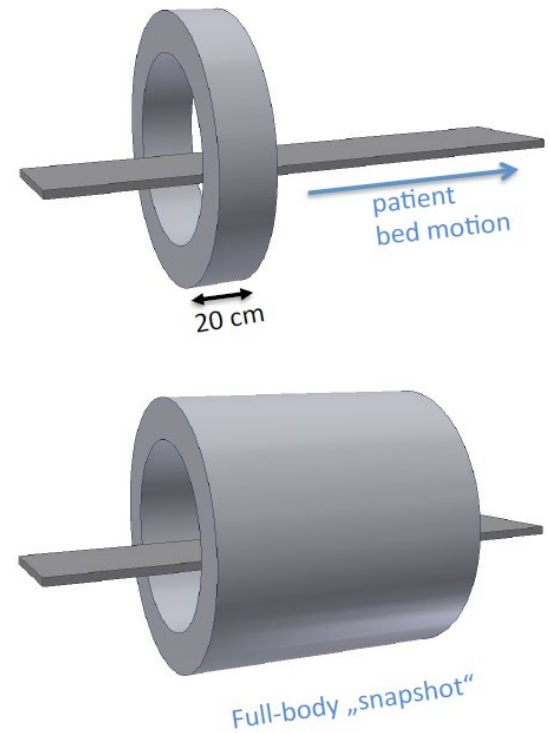


\*Theranostics is a two-pronged approach to diagnosing and treating cancers through the use of radiotracers. Radiotracers are compounds made of chemicals that selectively bind to a specific target in the body, and of a radiative component. In the diagnostic phase, the radioactive part is a beta emitter, while in the treatment phase it is a strong radiation source to damage the cancer cells.

# Current situation

---

- Standard clinical scanners are sub-optimal:
  - Cost of equipment, limited access, performance.
- Novel long axial PET scanners offer a very attractive solution in terms of
  - increased sensitivity and
  - enabling fast pharmacokinetics/pharmacodynamics.
- They pose significant challenges both
  - Financially
  - Logistically



# State-of-the-art in TOF PET

Essential parameter: CTR – coincidence timing resolution



- Clinical scanner:
  - Siemens Biograph Vision PET/CT → **214 ps**

<https://www.siemens-healthineers.com/molecular-imaging/pet-ct/biograph-vision>

- Laboratory measurement:
  - Gundacker *et al*, Phys. Med. Biol. 65 (2020) 025001 (20pp)  
 $2 \times 2 \times 3 \text{ mm LSO} \rightarrow \mathbf{58 \text{ ps}^*}$   
 $2 \times 2 \times 20 \text{ mm LSO} \rightarrow 98 \text{ ps}^*$

\*measured with single crystals with high-power readout electronics that cannot be scaled to large devices

# Gamma detectors for PET

---

Scintillating crystal:

- converts gamma energy into optical photons



Photodetector

- converts optical photons into electrical pulses

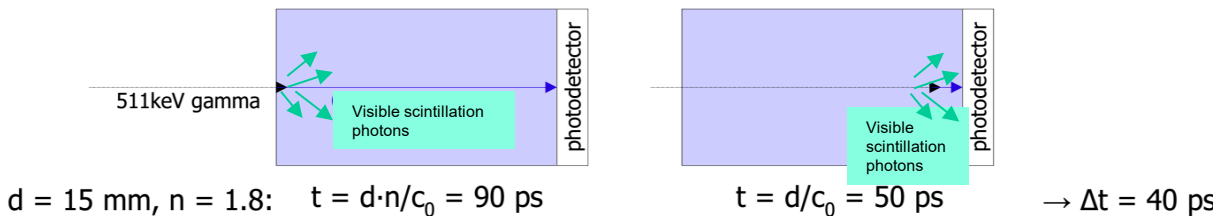
Time resolution in TOF PET limited by

- scintillation light emission → '10 ps challenge'
- rise and decay time
- **optical photon travel time spread in the crystal**
- **photodetector response**
- **readout electronics**

# Limitations on timing due to optical travel time

Inherent limitation for any crystal-based annihilation gamma detector:

- optical photons, produced in the crystal, need to reach the photodetector
- inside the crystal, **optical photons** propagate at a **lower speed** ( $c/n$ ) than **gamma rays** ( $c$ )
- refractive index, crystal dimensions → **intrinsic travel time spread** due to different gamma interaction depths
- for a 15 mm long crystal this contribution is  $> 40$  ps FWHM:



- Can in principle be corrected for by:
  - measuring the depth of interaction (DOI)
  - building the detector with shorter crystals → multi-layer configuration

# Can we simplify the TOF PET scanner

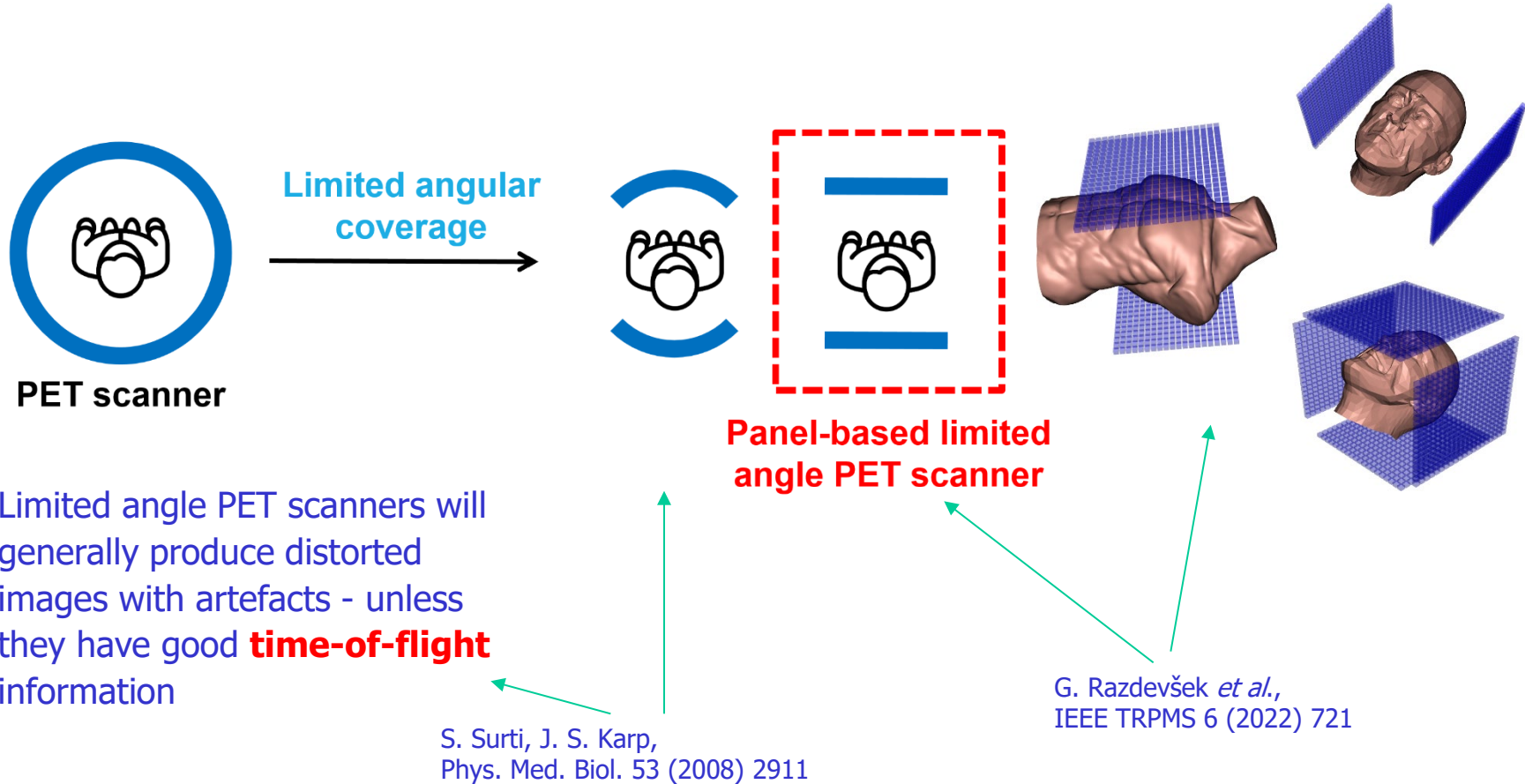
---

– and make it **cheaper** and **flexible**?



# Next generation scalable time-of-flight PET

Superb time resolution enables simplifications in the scanner design

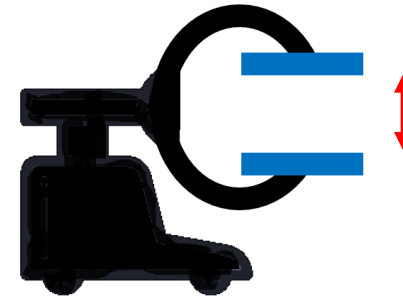


# Potential benefits of a panel-based PET system

---

## Mobility

- Portable or bedside PET imaging

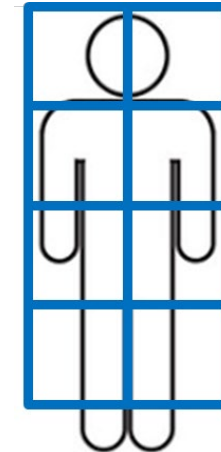


## Flexibility

- Adjustable FOV and sensitivity

## Modularity

- Combining multiple panels → multi-organ/total-body PET scanner



## Accessibility

- Reduced manufacturing cost and complexity

# Simulation of a limited angle system

**Geant4/GATE** → Monte Carlo simulations of digital phantoms and different scanner designs

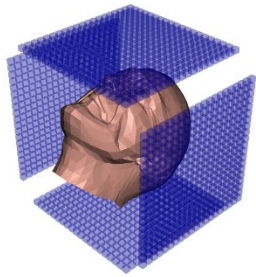


**CASToR** → image reconstruction with Maximum Likelihood Expectation Maximization (**MLEM**) algorithm

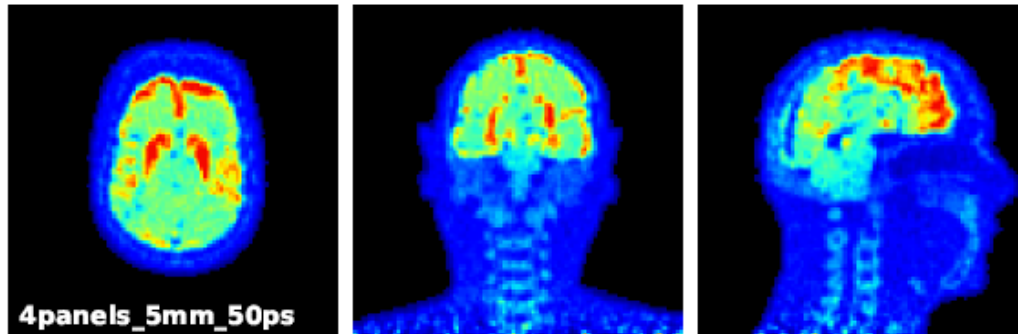
- Investigate the benefits of coincidence time resolution
- Study the performance **two-panel** and **four-panel** designs



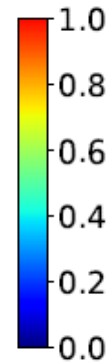
# Enabling Open Geometry systems



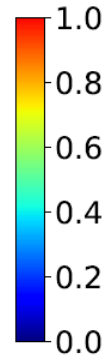
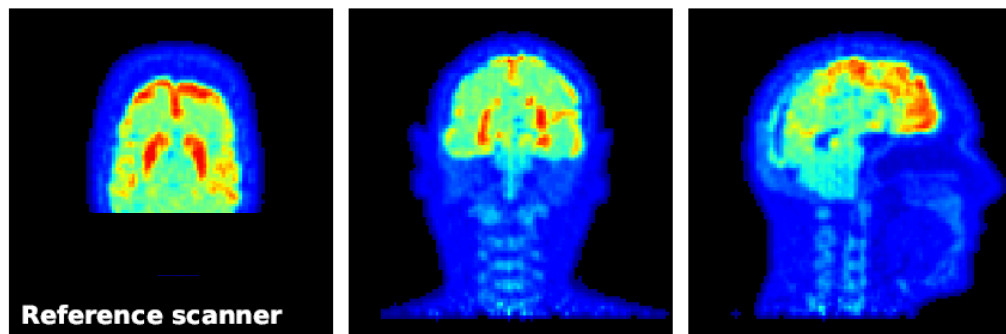
Two pairs of 30x30 cm<sup>2</sup>  
LYSO panels with 50ps CRT



Similar performance as 

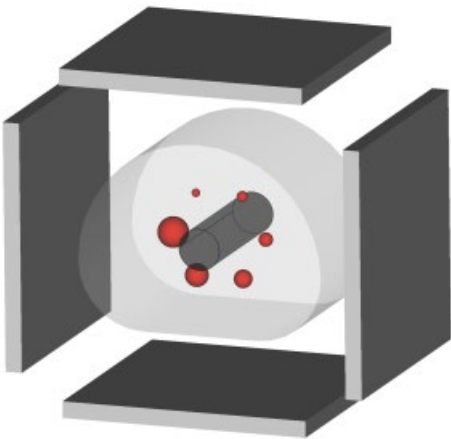


Siemens Biograph Vision

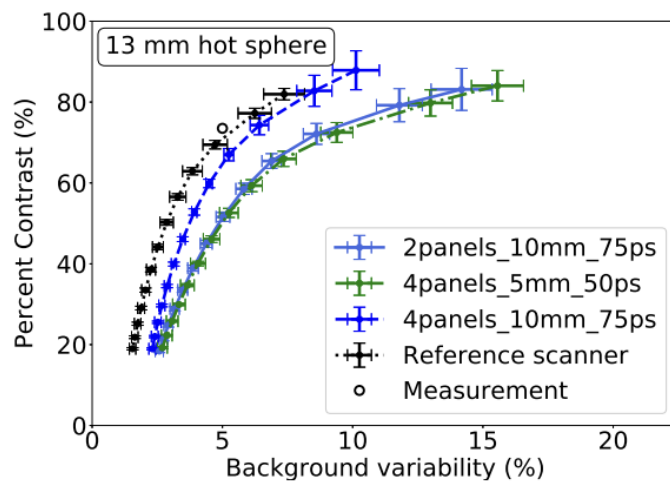


G. Razdevšek *et al.*, "Multi-panel limited angle PET system with 50 ps FWHM coincidence time resolution: a simulation study," IEEE TRPMS 6 (2022) 721, doi: 10.1109/TRPMS.2021.3115704.

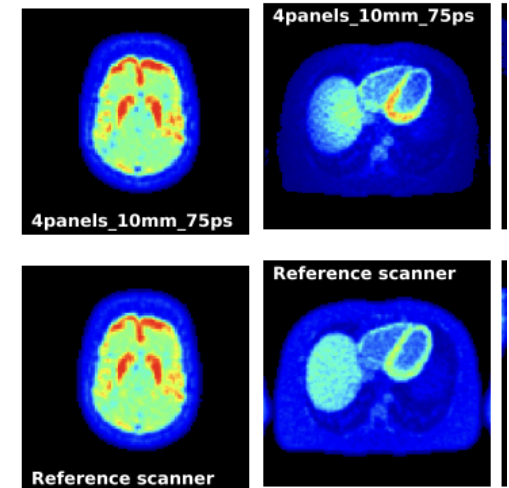
# Simulation study of planar configurations



Simulated arrangement  
of 30x30 cm<sup>2</sup> flat panel  
detectors



Percent contrast versus background  
variability (~noise level in the  
image)



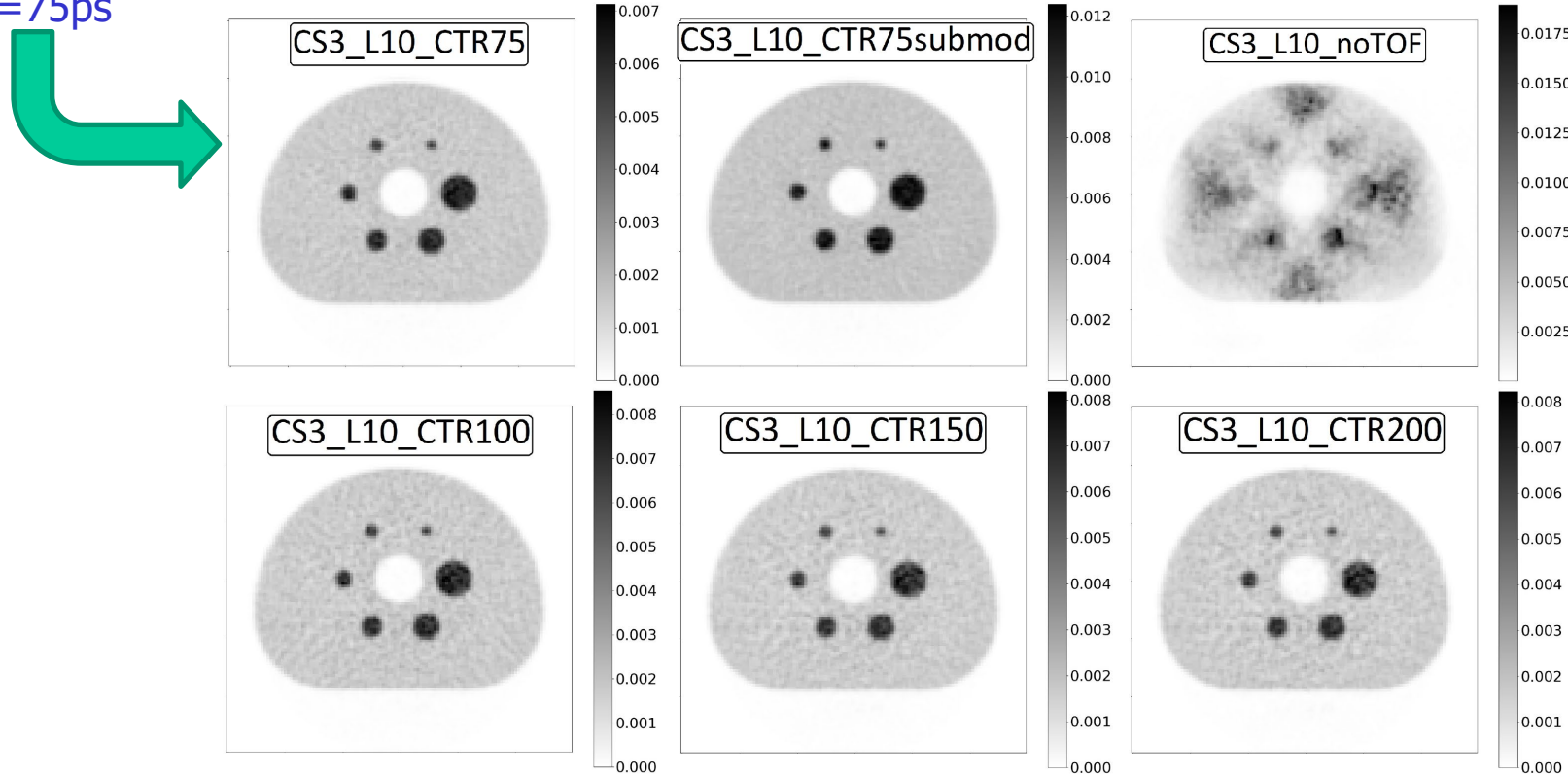
Reconstructed images of a  
torso and head for the flat  
panel detectors and the  
reference scanner Siemens BV

G. Razdevšek *et al.*, IEEE TRPMS 6 (2022) 721

# Design optimisation of a flat-panel, limited-angle TOF-PET scanner: simulation

Reconstructed NEMA phantom for various detector parameters.

Scanner: 3mm x 3mm x 10mm,  
CTR=75ps

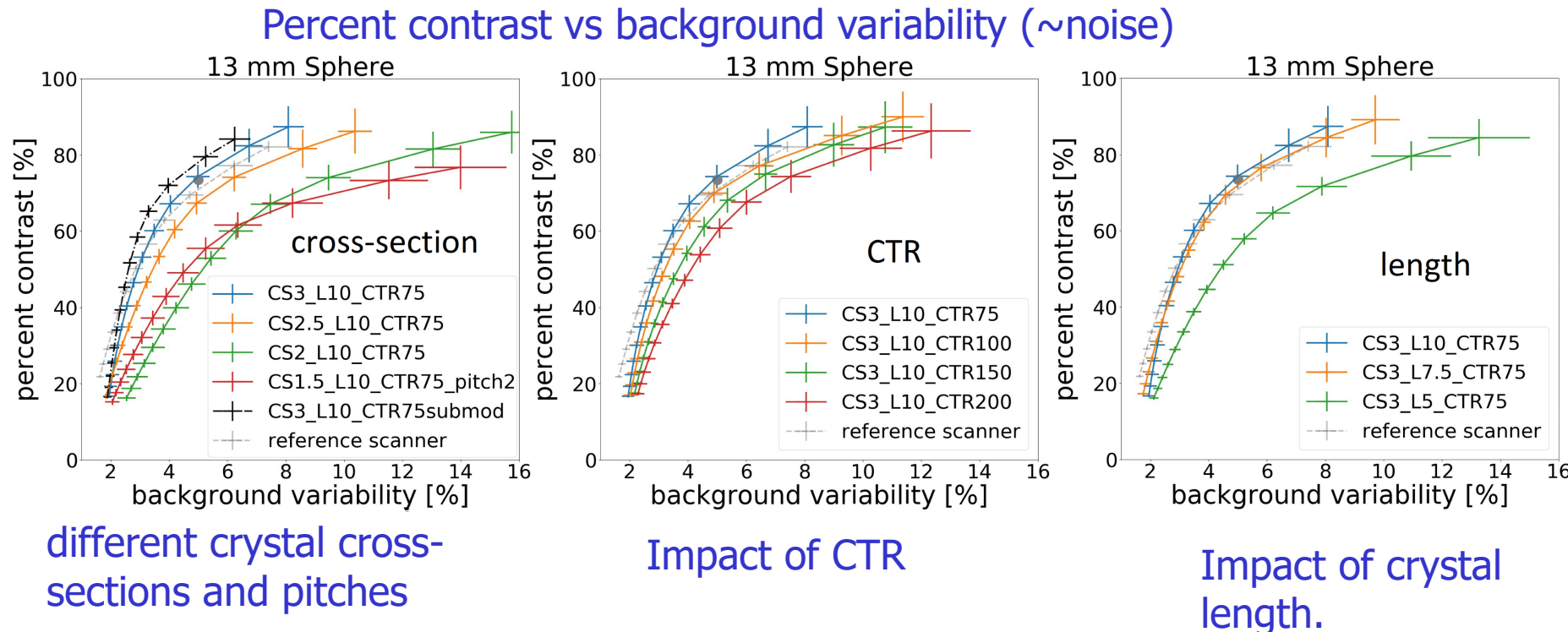


A 5 mm filter is applied to all of the images.

M. Orehar et al., Design Optimisation of a Flat-Panel, Limited-Angle TOF-PET Scanner: A Simulation Study. *Diagnostics* 14 (2024) 1976, doi: 10.3390/diagnostics14171976.

# Design optimisation of a flat-panel, limited-angle TOF-PET scanner: simulation

Image quality plots for the 13 mm sphere for different scanner parameters.



M. Orehar et al., Diagnostics 14 (2024) 1976

# Design optimisation of a flat-panel, limited-angle TOF-PET scanner: simulation

Images of the brain phantom in the transverse plane



activity phantom

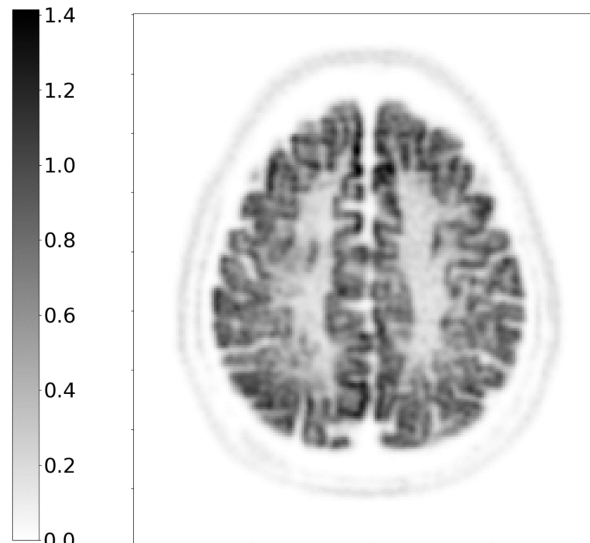


image reconstructed with the  
3mm x 3mm x 10mm, CTR 75ps  
scanner

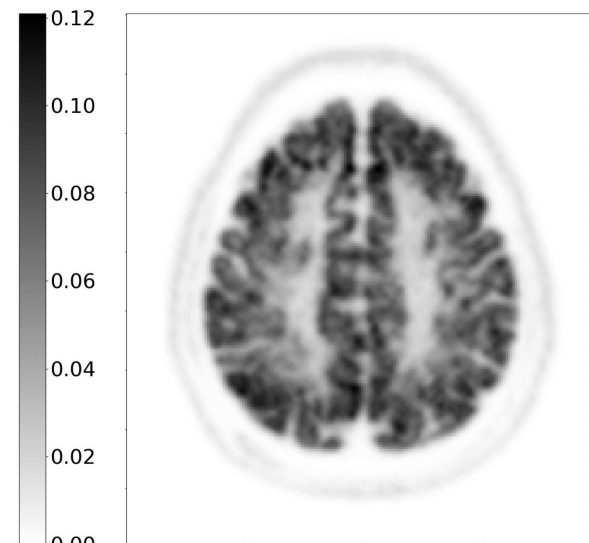
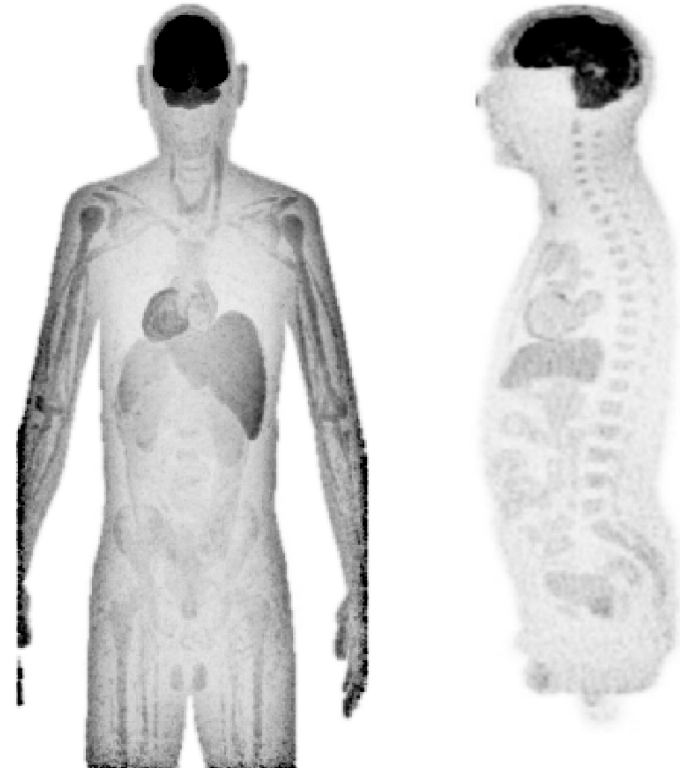
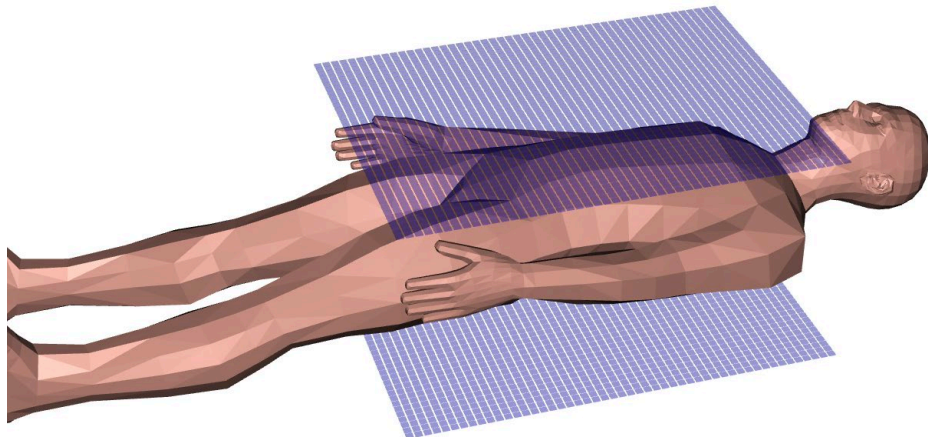


image reconstructed with  
the reference scanner.

M. Orehar et al., Diagnostics 14 (2024) 1976

# From Limited angle to Total-body

Increased sensitivity by larger panels



Capability of the planar TOF PET imager:

Image of a reconstructed 3 mm slice of a digital phantom acquired by two  $120 \times 60 \text{ cm}^2$  panel detectors (above and below the patient) assuming 100 ps TOF resolution and 10 mm LYSO scintillator thickness.

# Next-generation scalable time-of-flight PET

Address PET **system challenges** of a limited angular coverage using fast CTR

Joint effort: JSI, FBK, ICCUB, I3M, Oncovision, TU Munich and Yale

- Front-end electronics: develop a low-noise, high-dynamic-range ASIC with a time resolution of 20 ps & on-chip TDC
- Improve SiPM sensor
- Explore 2.5 D integration with the photo-sensor to achieve sub-100 ps CTR

Aim: Improve (SNR) without increasing cost associated with axial coverage by resorting to very sparse angular coverage of the patient and long axial field coverage

Managed to get a **3 MEUR EIC EU grant** for 5 years to further develop the method and construct a prototype.

PI: Rok Pestotnik (JSI)

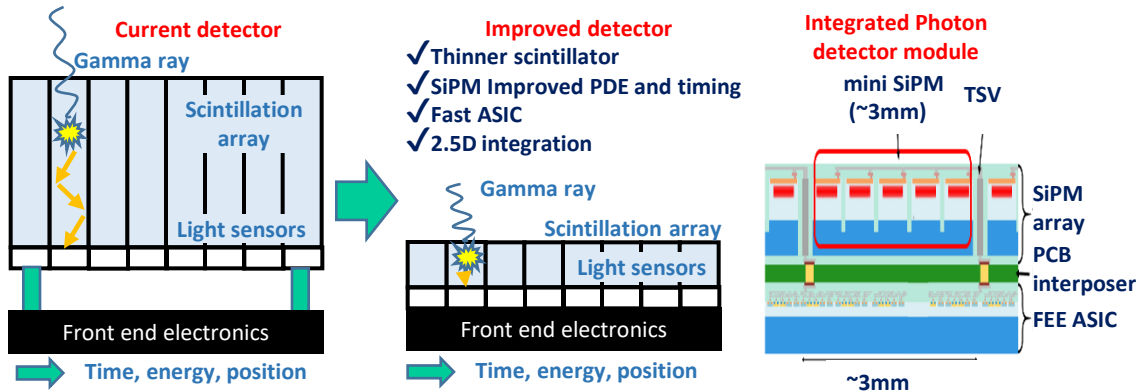
<https://petvision.org>



Supplemented by a recently awarded NIH grant to Yale.

# Fast CTR PET module

How to achieve such a good CTR?

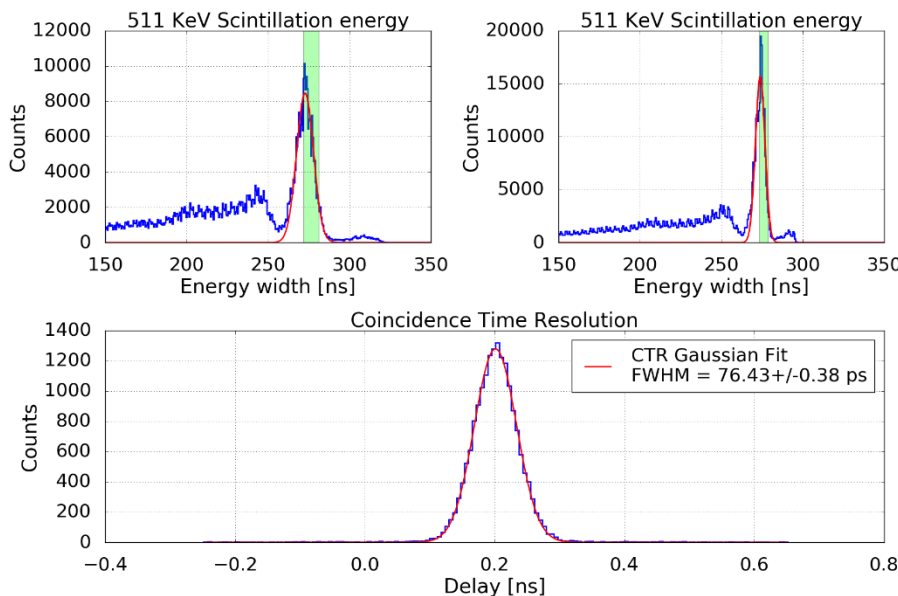


- Sensor: SiPM development at FBK
- FEE ASIC: FastIC, 8-channel ASIC for fast single photon sensors, a collaboration of ICCUB (Univ. Barcelona) and CERN

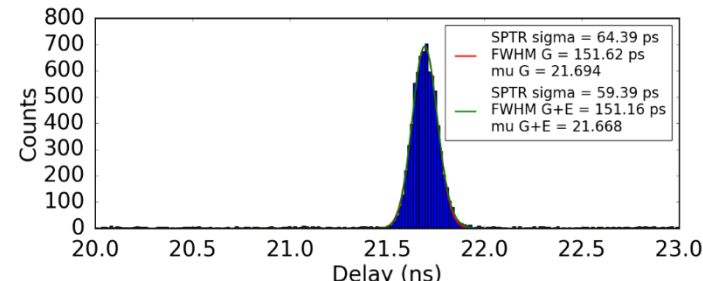
# First results with FastIC

- **Sensor:** FBK-NUVHDLFv2b 3x3 mm<sup>2</sup>, 40 pixel pitch.
- **Crystal:** LSO:Ce Ca 0.2% of 2x2x3 mm<sup>3</sup>.

Single photons



- **SPTR with FBK-NUVHDLFv2b 3x3**



FWHM = 76.43 ps

Pairs of annihilation gammas

D. Gascon, talk at Instrumentation for the future of particle, nuclear and astroparticle physics and medical applications in Spain, March 2023

- ICCUB and CERN are working on FastIC+: integration of 25 ps bin TDC on FastIC
- On the longer term plan for a 32 ch. ASIC (FastIC32)

# Limited angle PET scanner, conclusions

---

- Good coincidence time resolution can:
  - compensate for lower detection efficiency or smaller angular coverage
  - enable us to obtain **good image quality with a simple limited angle PET system** without distortions or artifacts
- We plan to enable open geometry designs and enable a wider spread of PET imaging by reducing different contributions to CTR :
  - Optimize scintillator thickness
  - Improve SiPM – TSV
  - Fast ASIC
  - 2.5D integration
  - If new – faster scintillators emerge, we should be able to make use of them

# Use of Cherenkov light in TOF-PET

---

## Use of Cherenkov radiation for TOF-PET

- lead fluoride ( $\text{PbF}_2$ ) as Cherenkov radiator material

## Previous work

## Limitations of Cherenkov TOF-PET

- single photon detection - **limited scatter suppression**

## Image quality with Cherenkov TOF-PET

- whole-body scanner simulations
- crystal readout configurations
- results

R. Dolenc<sup>a,b</sup>, D. Consuegra Rodríguez<sup>a</sup>, P. Križan<sup>a,b</sup>, M. Orehar<sup>b</sup>,  
R. Pestotnik<sup>a</sup>, G. Razdevšek<sup>b</sup>, A. Seljak<sup>a</sup> and S. Korpar<sup>a,c</sup>

<sup>a</sup> **J. Stefan Institute**, Ljubljana, Slovenia

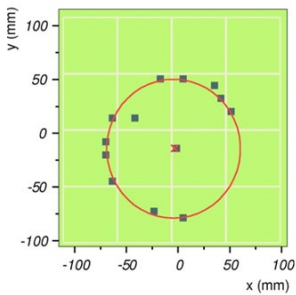
<sup>b</sup> Faculty of Mathematics and Physics, **University of Ljubljana**, Ljubljana, Slovenia

<sup>c</sup> Faculty of Chemistry and Chemical Engineering, **University of Maribor**, Slovenia

<https://photodetectors.ijs.si/>

# Imaging Cherenkov detectors

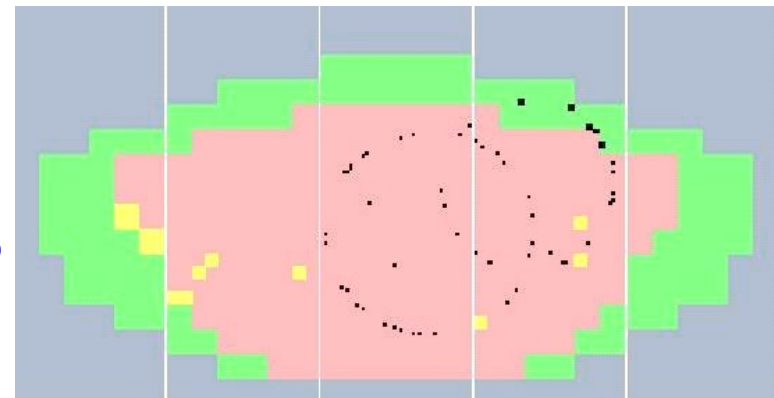
Measure the Cherenkov angle  
(RICH counter)



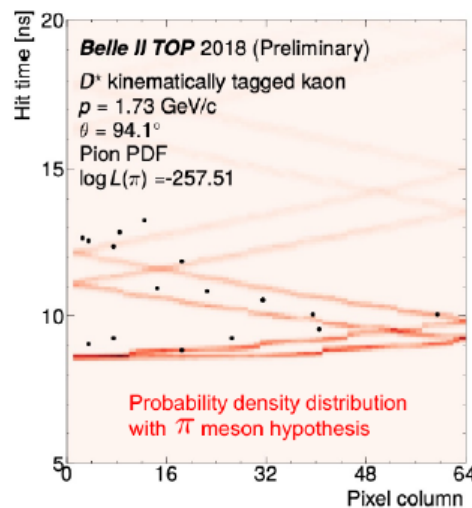
ARICH@Belle II



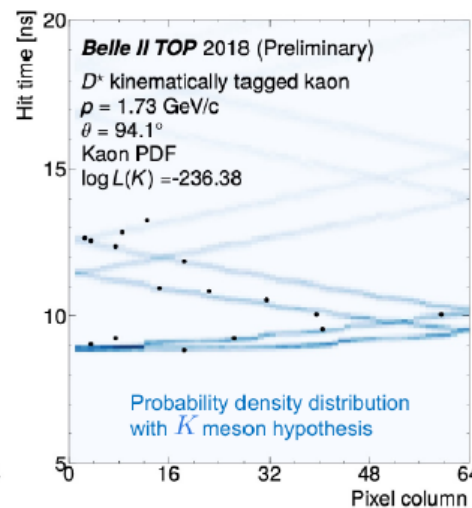
RICH@HERA-B



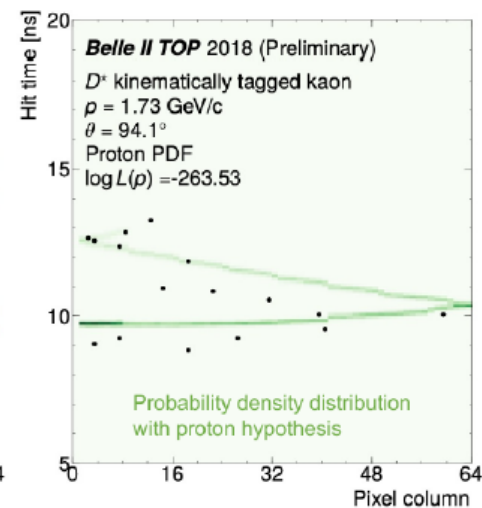
... or a pattern in  
the coordinate-  
vs-time space  
(TOP@Belle II)



Probability density distribution  
with  $\pi$  meson hypothesis



Probability density distribution  
with  $K$  meson hypothesis



Probability density distribution  
with proton hypothesis

# Use of Cherenkov Light in TOF-PET

$\gamma$  detectors in traditional PET: scintillator crystal + photodetector

Charged particles ( $e^-$  produced by  $\gamma$  interactions) passing through a dielectric material with  $v > c_0/n \rightarrow$  **prompt Cherenkov light**

Excellent Cherenkov radiator material: **lead fluoride ( $PbF_2$ )**

	BGO	LSO
Density (g/cm <sup>3</sup> )	7.1	7.4
$\mu_{511keV}$ (cm <sup>-1</sup> )	0.96	0.87
Photofraction for 511 keV	0.41	0.32
Raise time ( $\tau_r$ )	2.8 ns	70 ps
Decay time ( $\tau_d$ )	300 ns	40 ns
Light yield/511 keV (LY)	3,000	15,000

<b><math>PbF_2</math></b>
<b>7.77</b>
<b>1.06</b>
<b>0.46</b>
<b>10 (*)</b>

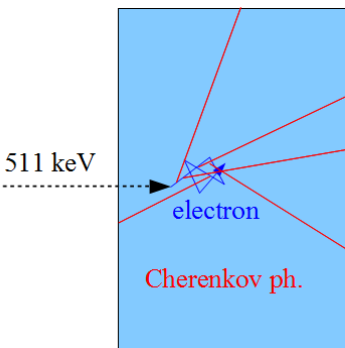
## $PbF_2$ properties.

- excellent  $\gamma$  stopping properties
- pure Cherenkov radiator (no scintillations)

(\*) in the 250-800 nm wavelength interval

- excellent optical transmission (down to 250 nm), high refractive index ( $n \sim 1.8$ )
- low price (**1/3 BGO, 1/9 LSO**)

Mao, IEEE TNS 57:6 (2010) 3841

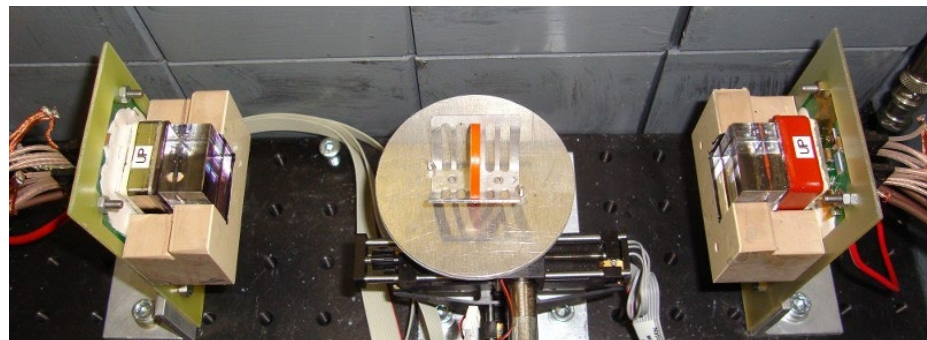


# TOF-PET with Cherenkov light detection: proof of principle

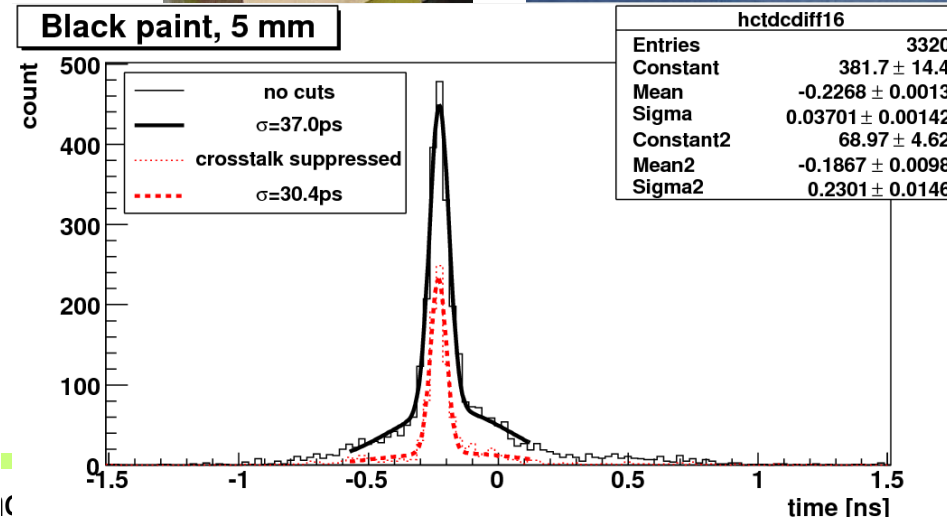
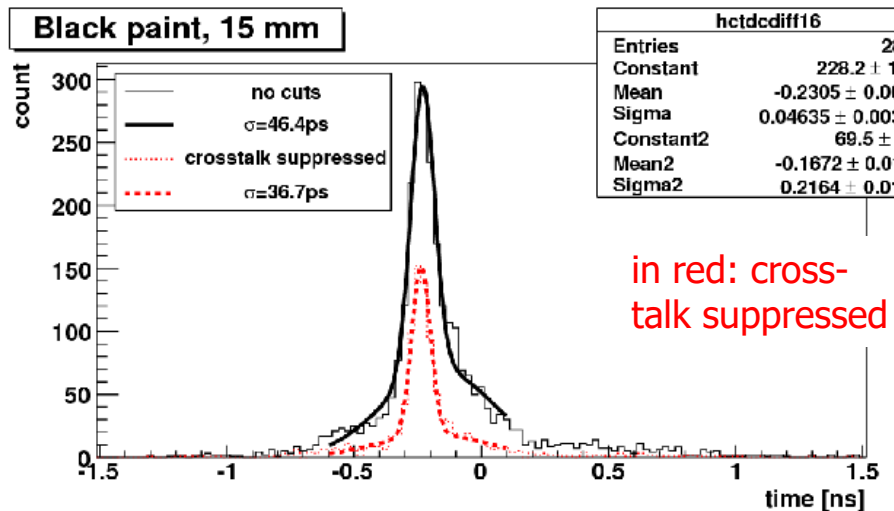
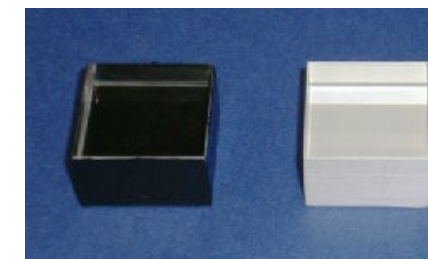
Two detectors (back-to-back)

- 25 x 25 x 15 mm<sup>3</sup> crystals (black painted or Teflon wrapped)
- MCP-PMT (Hamamatsu, same as in the Belle II TOP counter)
- <sup>22</sup>Na source

S. Korpar et al, NIM A654 (2011) 532



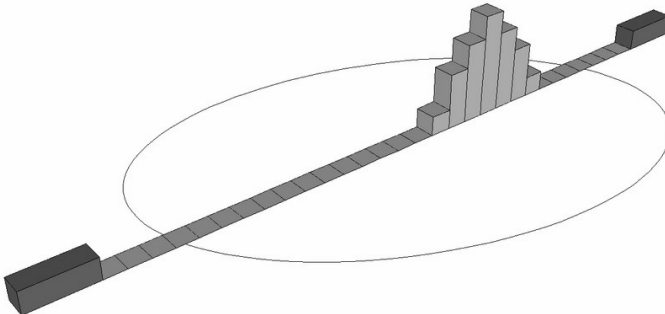
- 15 mm long crystal: FWHM  $\sim$  95 ps
- 5 mm long crystal: FWHM  $\sim$  70 ps



# Point source position

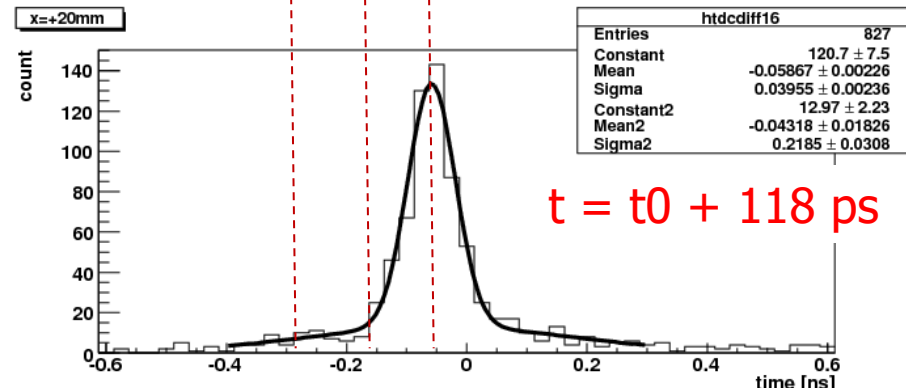
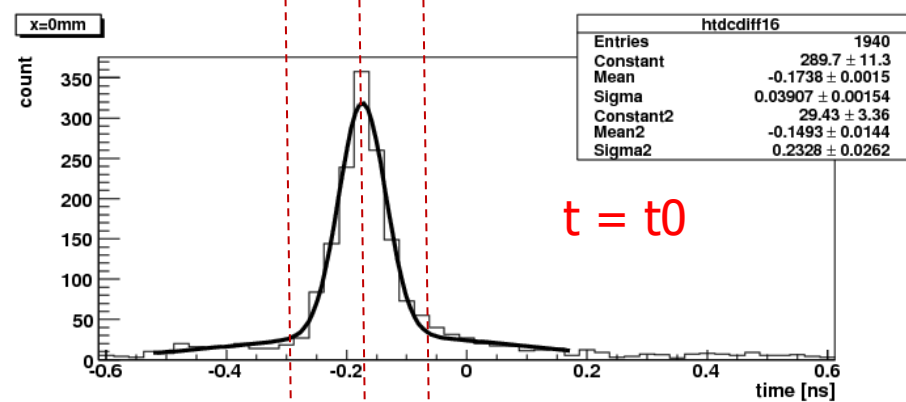
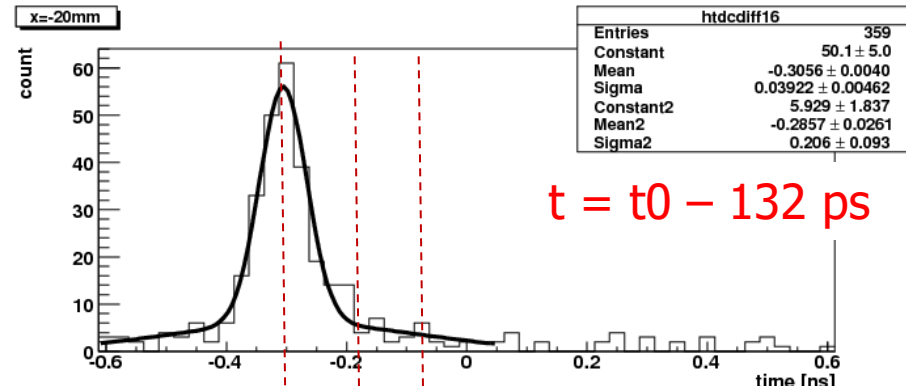
Data taken at three  $^{22}\text{Na}$  point source positions spaced by 20 mm:

- average time shift 125 ps
- timing resolution  $\sigma \sim 40$  ps rms,  
 $\sim 95$  ps FWHM
- position resolution along the line of response  $\sigma \sim 6$  mm rms,  
 $\sim 14$  mm FWHM



Black painted 15 mm  $\text{PbF}_2$  crystals.

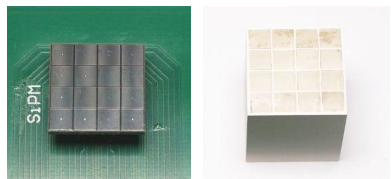
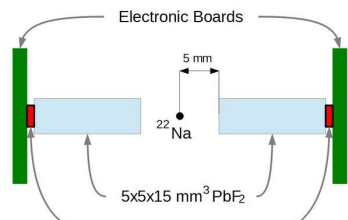
S. Korpar et al, NIM A654 (2011) 532



# Some results of our studies

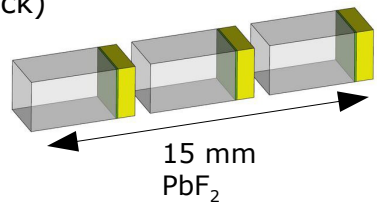


$(25 * 25 * 15)$  mm<sup>3</sup> **PbF<sub>2</sub>** (black)  
+  $(22.5 * 22.5)$  mm<sup>2</sup> **MCP-PMT**



**4x4 array:**  
 $(3 * 3 * 15)$  mm<sup>3</sup> **PbF<sub>2</sub>** (reflector)  
+  $(3 * 3)$  mm<sup>2</sup> **SiPM**

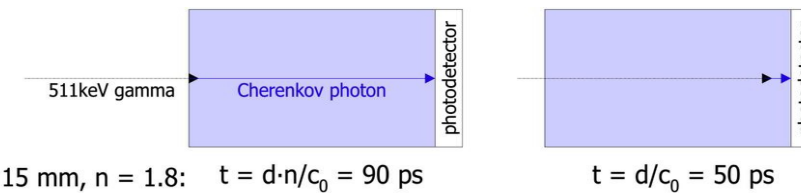
**Multi-layer: 3 x**  
[( $3 * 3 * 5$ ) mm<sup>3</sup> **PbF<sub>2</sub>** (black)  
+  $(3 * 3)$  mm<sup>2</sup> **SiPM**]



Result	Reference
Cherenkov TOF PET, TOF: <b>95 ps</b> FWHM	Korpar, NIM A 654 (2011) 532
With SiPMs, TOF: <b>306 ps</b> FWHM	Dolenec, IEEE TNS 63:5 (2016) 2478
Cherenkov PET module: Single side efficiency: <b>35 %</b>	Dolenec, NIM A 952 (2020) 162327
Multi-layer detector (simulation) TOF: <b>22 ps</b> FWHM before photodetector timing	Consuegra, Phys. Med. Biol. 65(5) (2020) 055013

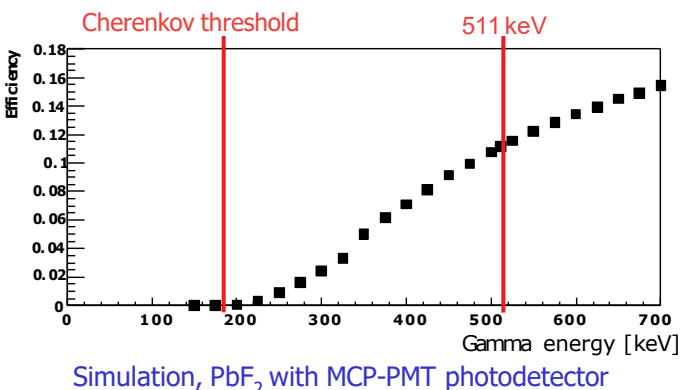
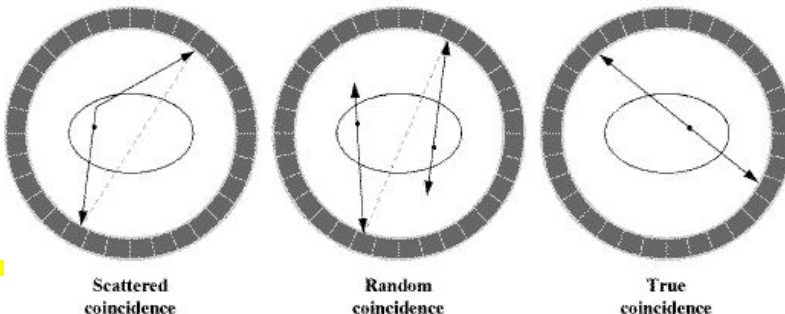
# Limitations of Cherenkov TOF-PET

- Only 10-20 photons created → **only a few detected**
  - efficient photodetector and light collection needed
- Optical photon travel time spread** in the crystal
  - remaining limitation to TOF resolution



- Limited suppression of **scattered events**:
  - only a few Cherenkov photons detected  
→ no energy information
  - detection efficiency drops at low gamma energies  
→ intrinsic suppression

## Effect of remaining scatter on image quality?



Essential question → MC simulation to evaluate the effect



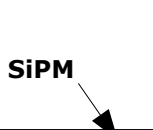
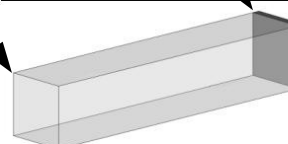
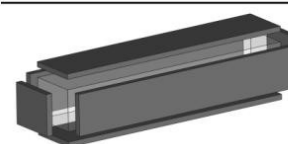
# Crystal readout configurations

## Simulation:

- Cherenkov photon generation, propagation simulated
- Timing defined by first optical photon detected

### Reference scanner

- LSO scintillator
- Energy window: 435-585 keV
- Energy resolution: 10%
- CTR: 214 ps

	Cherenkov detector	Surface treatment	$\epsilon^2$ (%)	CTR-FWHM (ps)		FOM	
				0 ps SPTR	70 ps SPTR	0 ps SPTR	70 ps SPTR
	1-sided-back	Black	8.6	100.7	145.5	0.85	0.59
		Reflector	35.3	135.7	184.8	2.60	1.91
	2-sided-top-bottom	Black	26.2	47.0	111.1	5.57	2.36
		Reflector	40.5	48.9	117.8	8.28	3.44
	6-sided	/	44.4	54.1	115.4	8.21	3.85

Coincidence detection efficiency:  $\epsilon^2$

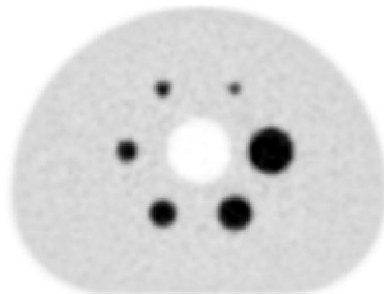
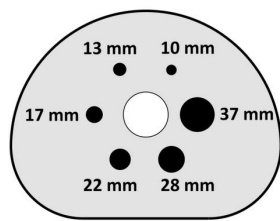
Figure-of-merit:  $FOM = \frac{\epsilon^2}{CTR}$

G. Razdevšek *et al.*, "Exploring the Potential of a Cherenkov TOF PET Scanner: A Simulation Study," IEEE TRPMS 7 (2023) 52, doi: 10.1109/TRPMS.2022.3202138.

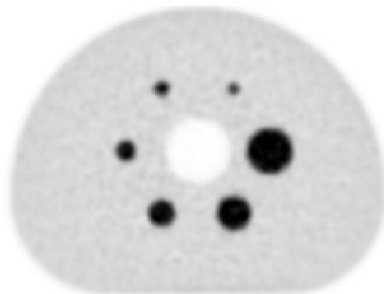
SPTR = single photon time resolution

# Results: Image Quality

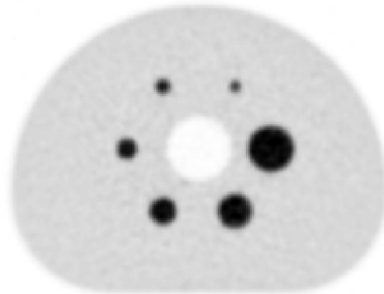
## NEMA image quality phantom



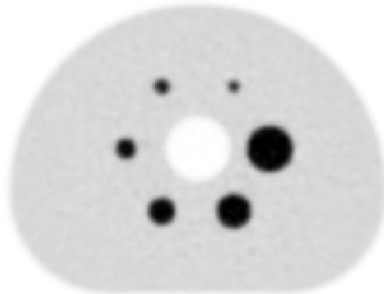
Reference-scanner-214ps



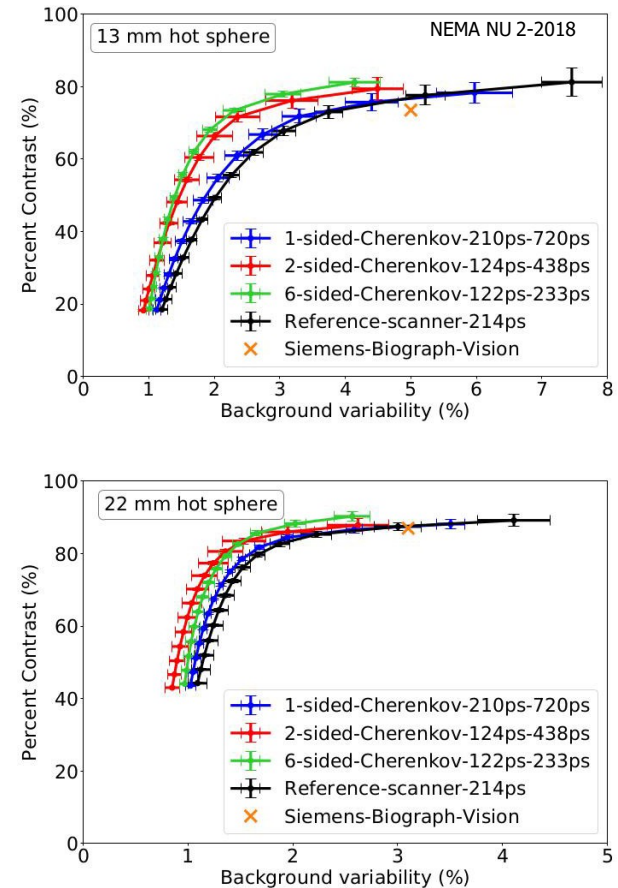
1-sided-210ps-720ps



2-sided-124ps-438ps



6-sided-122ps-233ps



Better sensitivity and CTR compensate for higher scatter fraction

Image quality comparable to state-of-the-art

G. Razdevšek *et al.*, IEEE TRPMS 7 (2023) 52

# Hybrid Cherenkov-scintillator approach

Cherenkov light is also produced in scintillator materials

- BGO: low cost, high density, historically used for PET

The idea:

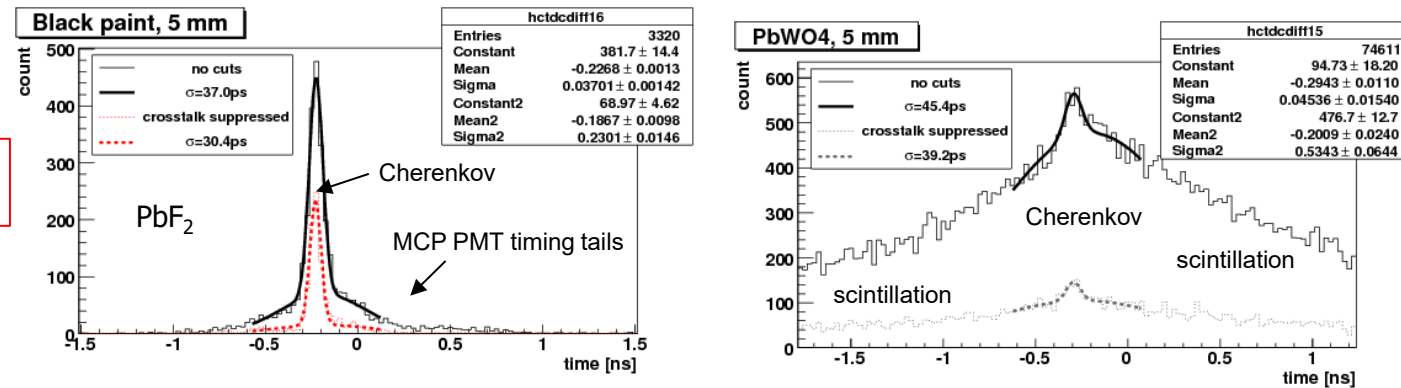
- use (abundant) scintillation light for energy measurement/photopeak cut
- use the few Cherenkov photons for timing

Issues:

- few coincidences formed by detection of Cherenkov photons on both sides
- → long tails in CTR distribution, how to handle them in reconstruction?
- does not look very promising

Measured CTR with  $\text{PbF}_2$  vs.  $\text{PbWO}_4$  scintillator:

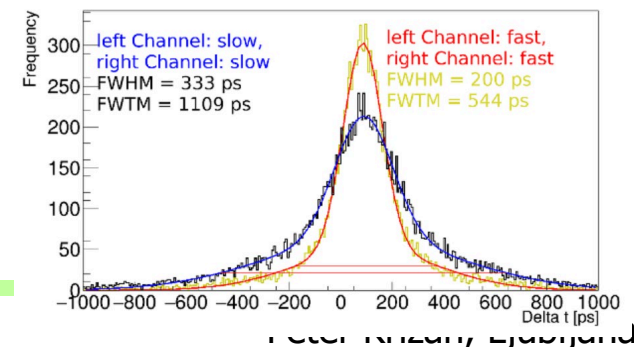
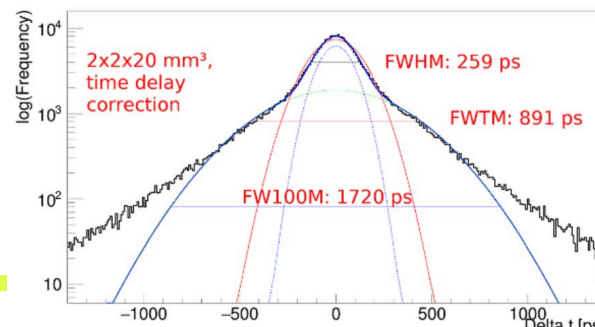
S. Korpar, NIM A 654 (2011) 532



Measured CTR with BGO:

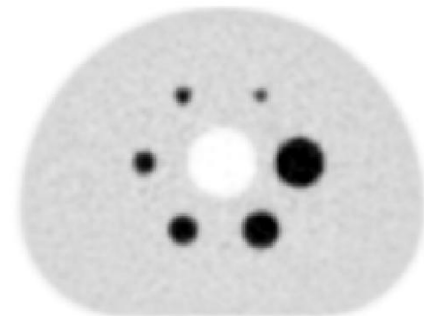
N. Kratochwil et al.,  
Phys. Med. Biol. 65 (2020) 115004

N. Kratochwil et al.,  
IEEE TRPMS 5(5) (2020) 619-629

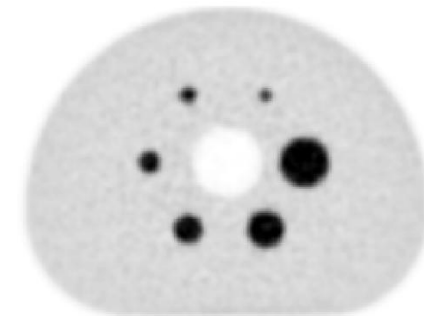


# Cherenkov based scanners, conclusion

- Using (exclusively) Cherenkov light in TOF-PET has potential to
  - improve TOF resolution
  - reduce scanner cost (total-body)
- Experiments have demonstrated
  - CTR as low as 30 ps [R. Ota, Phys. Med. Biol. 64 \(2019\) 07LT01](#)
  - detection efficiency (module) of 35% [R. Dolenc et al, NIM A 952 \(2020\) 162327](#)
- Cherenkov TOF-PET scanner simulations
  - better sensitivity and CTR compensate for higher scatter fraction
  - **image quality comparable to state-of-the-art**
- Advanced detector geometries (2-sided top-bottom, multi-layer)
  - even better image quality



Reference-scanner-214ps



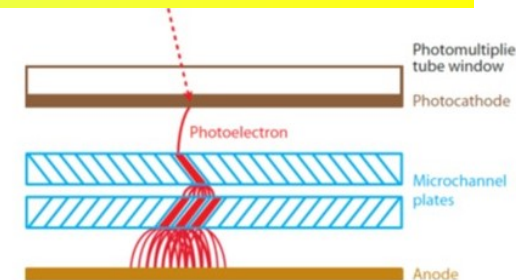
1-sided-210ps-720ps

[G. Razdevšek et al., IEEE TRPMS 7 \(2023\) 52](#)

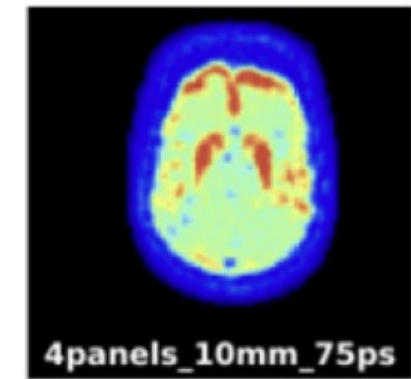
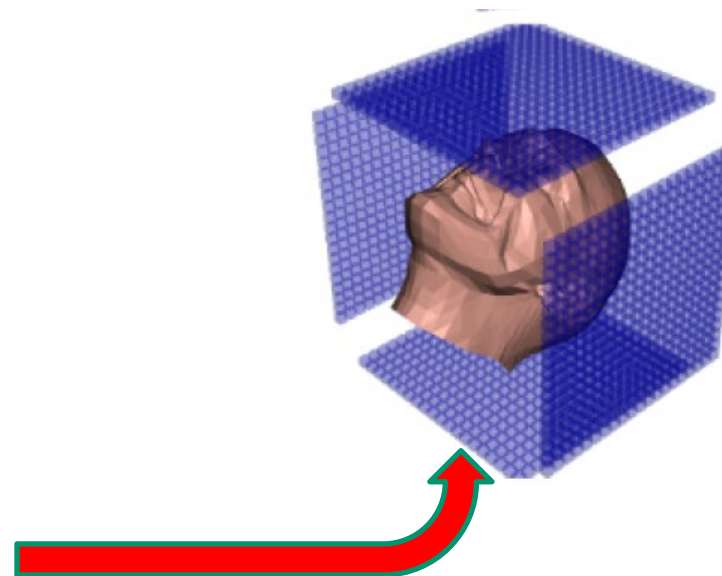
# Cherenkov-based TOF-PET with a large area MCP-PMT

Idea:

- couple short  $\text{PbF}_2$  crystals as Cherenkov radiators to the
- LAPPD – a large area MCP-PMT, and make use of the
- flat panel concept



LAPPD with  $\text{PbF}_2$  crystals



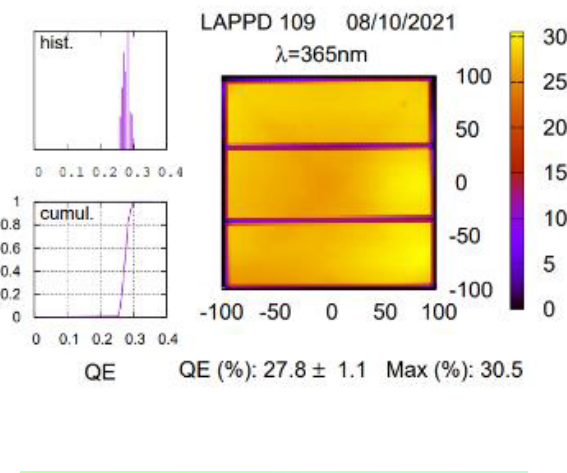
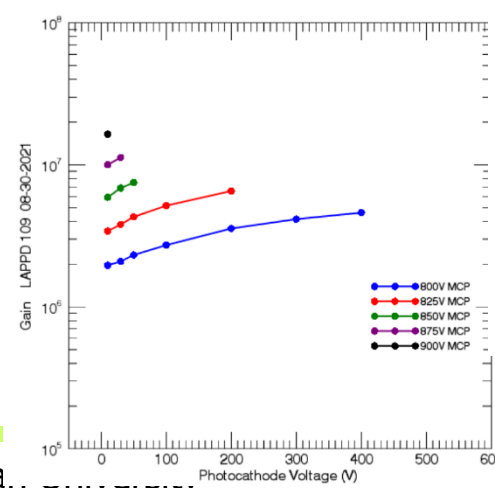
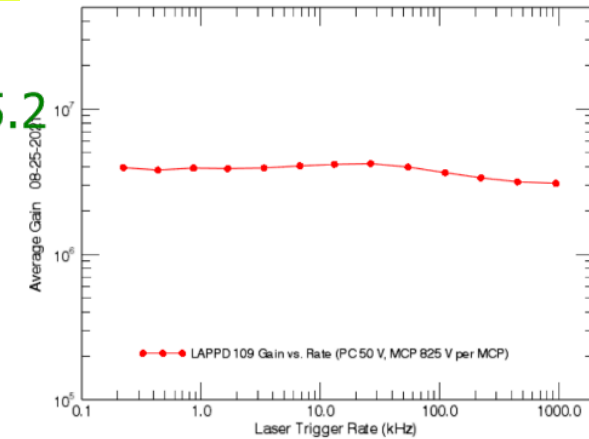
CherPET: an ERC (European Research Council) Proof-of-Principle project

LAPPD with  $\text{PbF}_2$  crystals attached to the entry window: an almost ideal flat panel device

# LAPPD (large area picosecond photodetector) Gen II

## Characteristics (Incom):

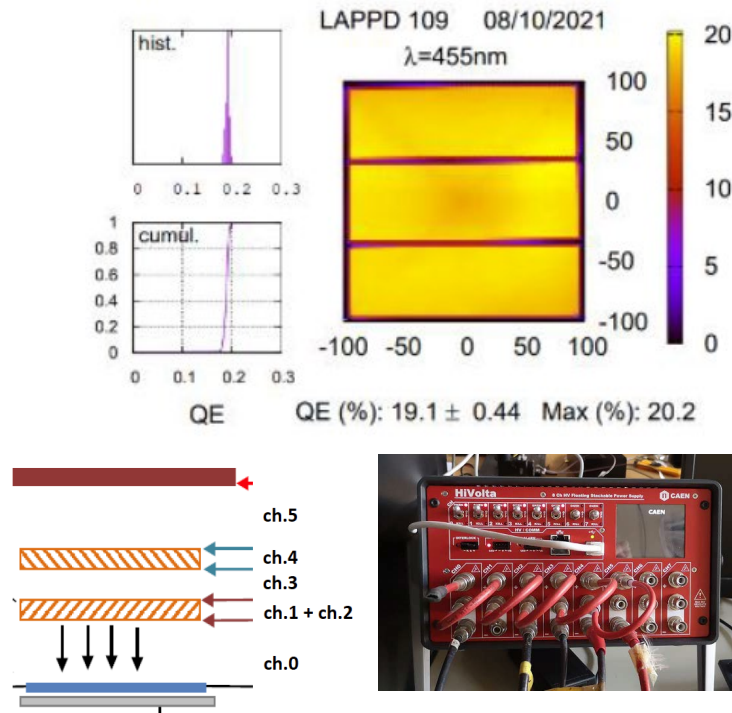
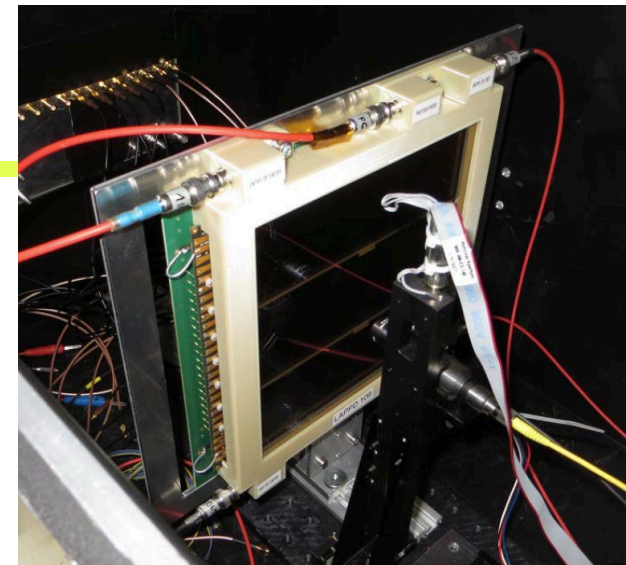
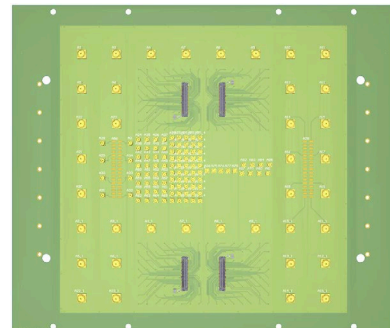
- size  $230 \text{ mm} \times 220 \text{ mm} \times 22 \text{ mm}$  ( $243 \text{ mm} \times 274 \text{ mm} \times 25.2 \text{ mm}$  with mounting case)
- borosilicate back plate with interior resistive ground plane anode – 5 mm thick
- capacitively coupled readout electrode
- MCPs with  $20 \mu\text{m}$  pores at  $20 \mu\text{m}$  pitch
- two parallel spacers (active fraction  $\approx 97 \%$ )
- gain  $\approx 5 \cdot 10^6$  @ ROP (825 V/MCP, 100 V on photocathode)
- peak QE  $\approx 25\%$
- Dark Count rate @ ROP:  $\sim 70 \text{ kHz/cm}^2$  with  $8 \times 10^5$  gain



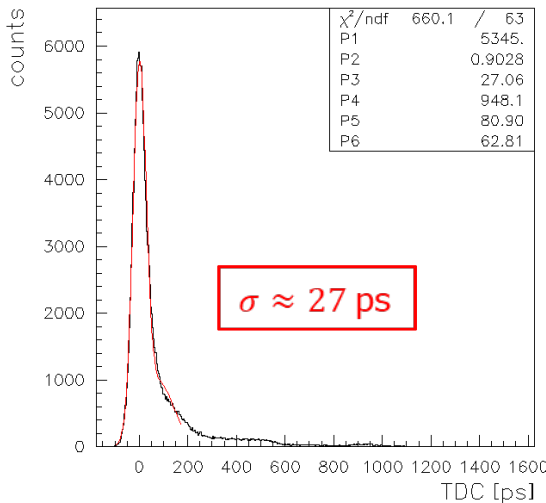
# LAPPD evaluation

- Two 10  $\mu\text{m}$  devices acquired
- LAPPD installed in the dark box:
- CAEN HiVolta (DT1415ET), 8 Ch Reversible 1 kV/1 mA Desktop HV Power Supply – floating channels
- Standard setup with QDC, TDC, 3D stage ...
  - TDC value corrected for time-walk
- ALPHALAS PICOPOWER™-LD Series of Picosecond Diode Lasers – 405 nm
  - FWHM  $\approx$ 20ps
  - light spot diameter on the order of  $100\mu\text{m}$
- Measure response in the lab with modular electronics, FastIC and PETSys
- Custom segmentation

to study the capacitive coupling and the charge spread



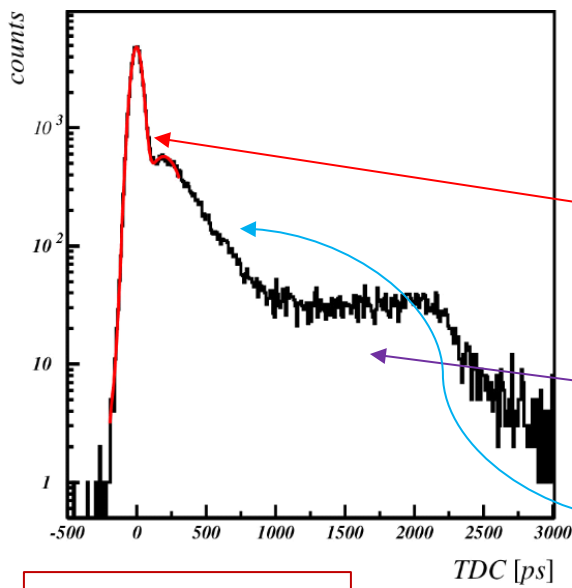
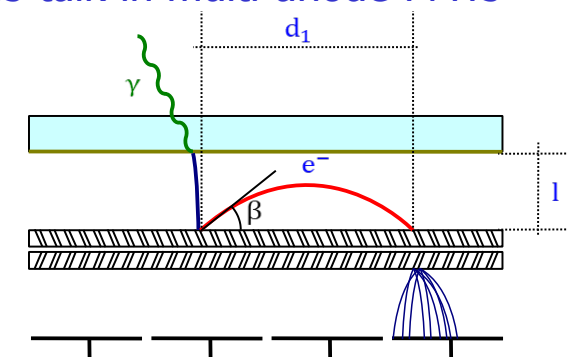
# Characterizing LAPPD: time resolution



Photoelectron back-scattering produces a rather long tail in timing distribution and position resolution.

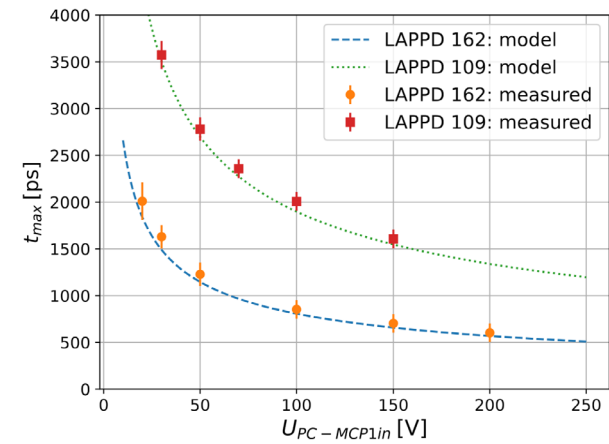
Photoelectron backscattering reduces collection efficiency and gain, and contributes to cross-talk in multi-anode PMTs

R. Dolenec *et al.*, NIM A 1069 (2024) 169864



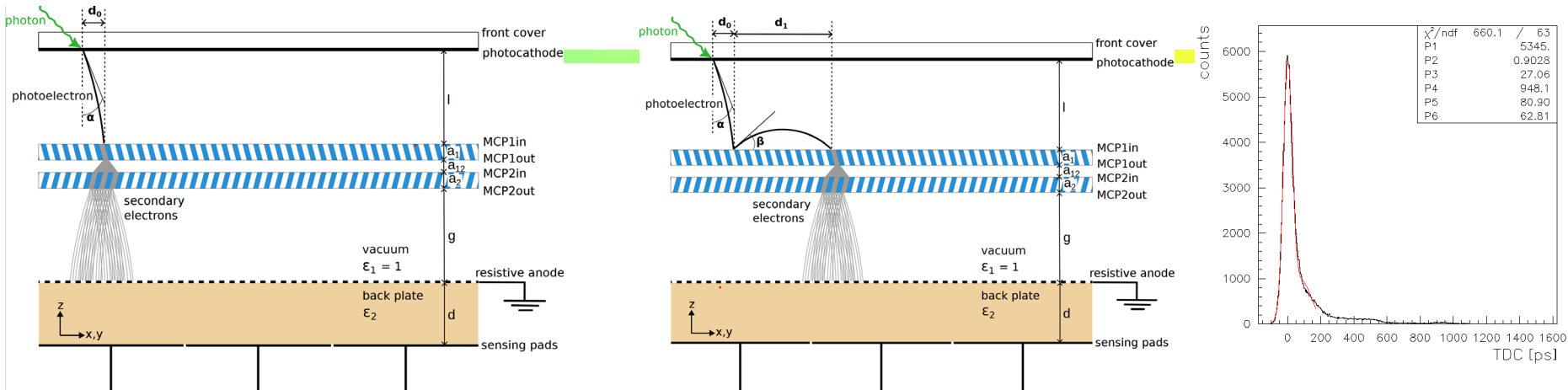
Typical single photon timing distribution with a narrow main peak ( $\sigma \sim 30$ -40 ps) and contributions from photoelectron elastic back-scattering (flat distribution) and inelastic back-scattering.

S.Korpar et al, PD07



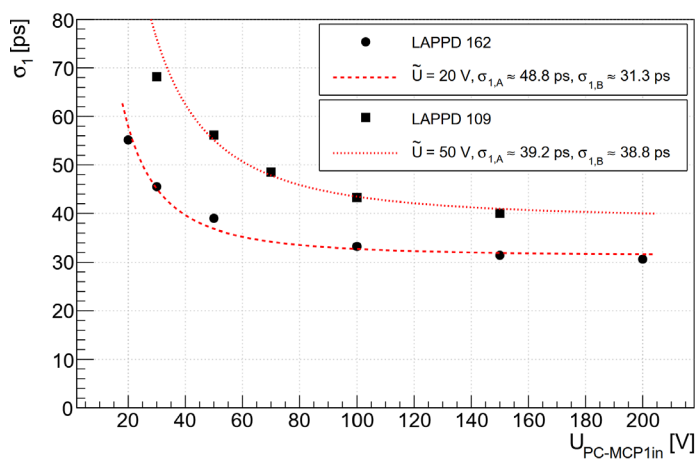
S.Korpar et al, arXiv:2406.19421[physics.ins-det] submitted to NIMA

# Characterizing LAPPD: time resolution and charge sharing

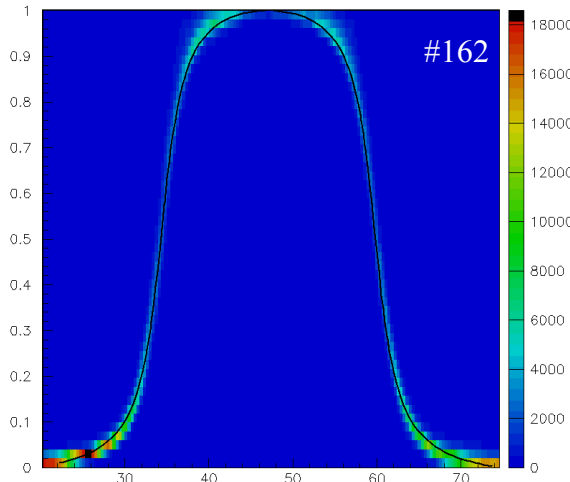


$\sigma$ (ps)

Time resolution vs  
PC-MCP1 voltage  $U$



S.Korpar et al, arXiv:2406.19421[physics.ins-det] submitted to NIMA



Charge sharing – capacitively coupled read-out electrodes. Black: model prediction, using Shockley-Ramo theorem.

Next steps: finalize read-out, attach crystals, test the back-to-back configuration

# Summary

---

The interplay of detector R&D for particle physics and medical imaging has a long history, and this will remain one of the sources of innovation in medical imaging.

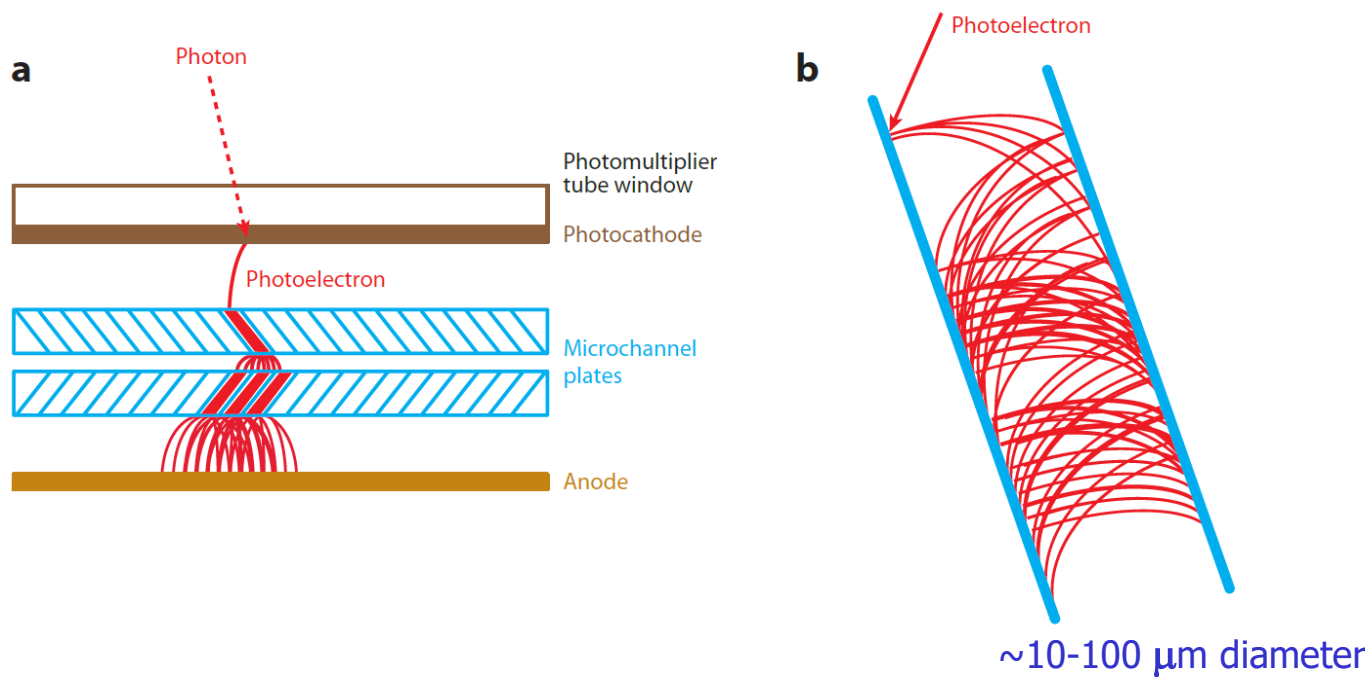
Limited angle devices with very fast gamma detection look very promising – lower cost, flexibility in use, affordable total-body scanner.

Cherenkov radiation based annihilation gamma detectors offer a promising method for very fast detection and potentially cheaper devices.

# More slides

---

# Micro Channel Plate PMT (MCP-PMT)



Multiplication step: a continuous dynode – a micro-channel coated with a secondary emitter material

# Micro Channel Plate PMT (MCP-PMT)

Similar to ordinary PMT – the dynode structure is replaced by MCPs.

Basic characteristics:

- Gain  $\sim 10^6$   $\rightarrow$  single photon
- Collection efficiency  $\sim 60\%$
- Small thickness, high field  $\rightarrow$  small TTS
- Works in magnetic field
- Segmented anode  
 $\rightarrow$  position sensitive



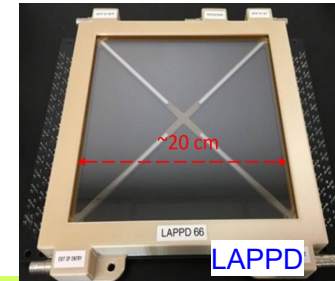
PHOTONIS



PHOTEK



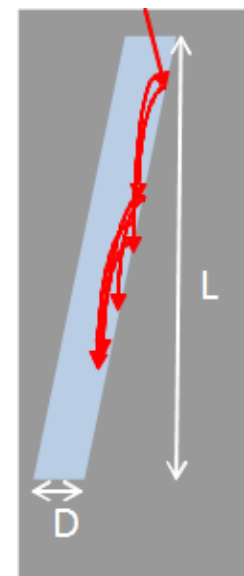
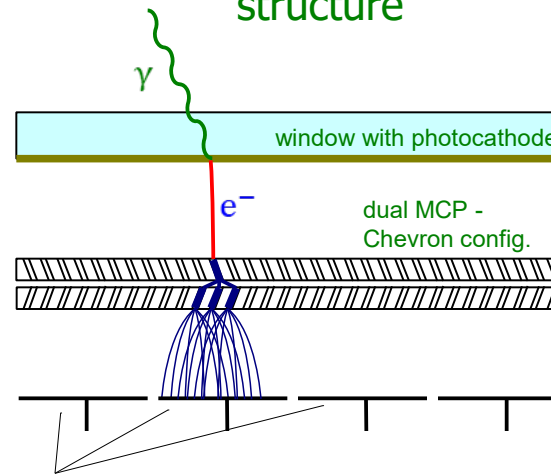
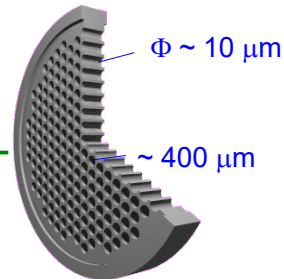
HAMAMATSU



LAPPD 66

$\sim 20$  cm

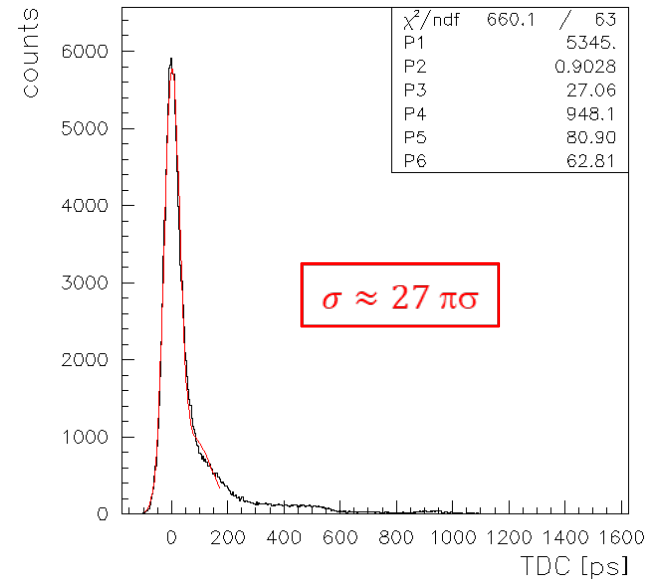
MCP is a thin glass plate with an array of holes ( $<10-100$   $\mu\text{m}$  diameter) -  
- a continuous dynode structure



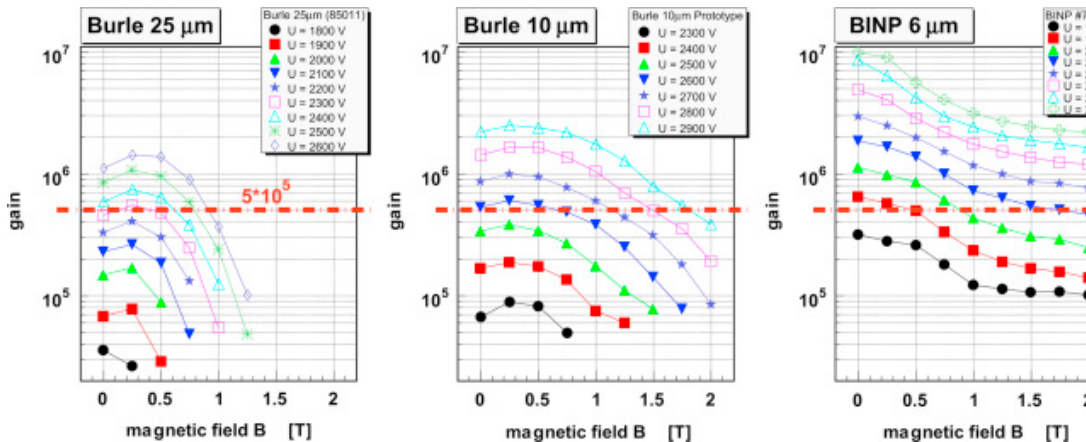
MCP gain depends on L/D ratio – typically 1000 for L/D=40

# Micro Channel Plate PMT: properties

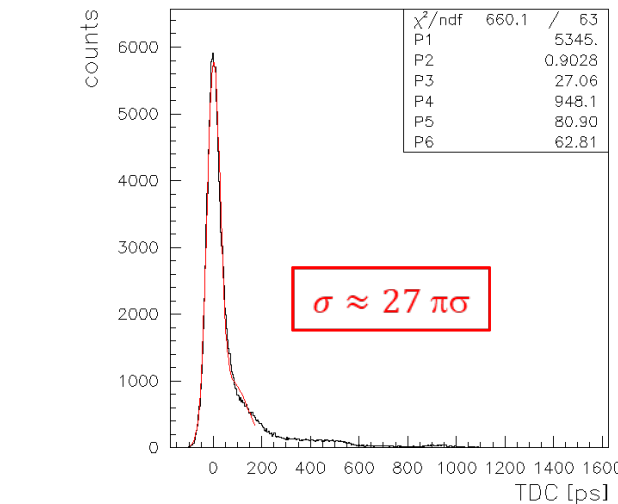
Very fast: single photon detection  
with sigma of  $\sim 30\text{-}40$  ps



MCP PMTs work well in magnetic fields  
→ performance depends on the diameter of the micro-channels

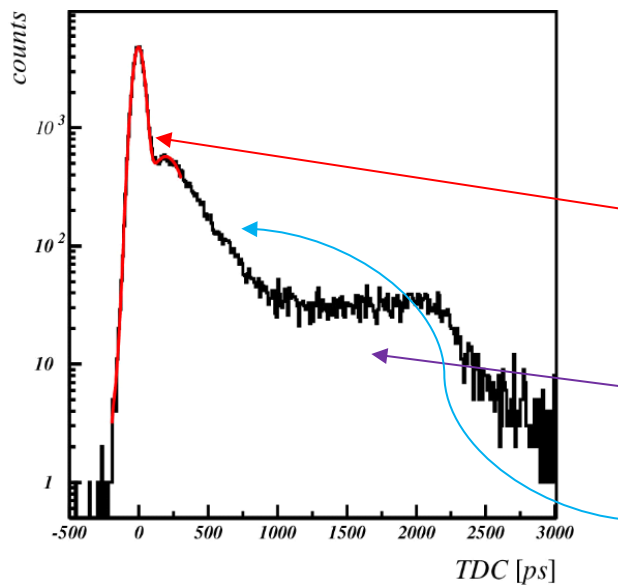


# MCP-PMT: single photon pulse height and timing

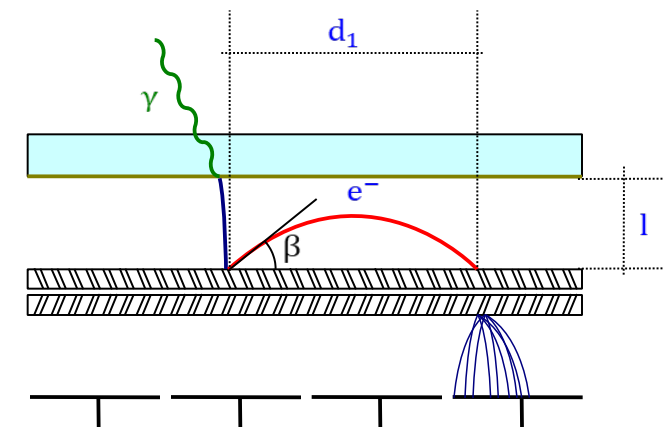


Photoelectron back-scattering produces a rather long tail in timing distribution and position resolution.

Photoelectron backscattering reduces collection efficiency and gain, and contributes to cross-talk in multi-anode PMTs



Typical single photon timing distribution with a narrow main peak ( $\sigma \sim 30$ -40 ps) and contributions from photoelectron elastic back-scattering (flat distribution) and inelastic back-scattering.



S.Korpar@PD07

# Modelling MCP-PMT: Photoelectrons in a uniform electric field

Photoelectrons travel from the photocathode to the electron multiplier (uniform electric field  $\frac{U}{l}$ , initial energy  $E_0 \ll Ue_0$ ):

- photoelectron range

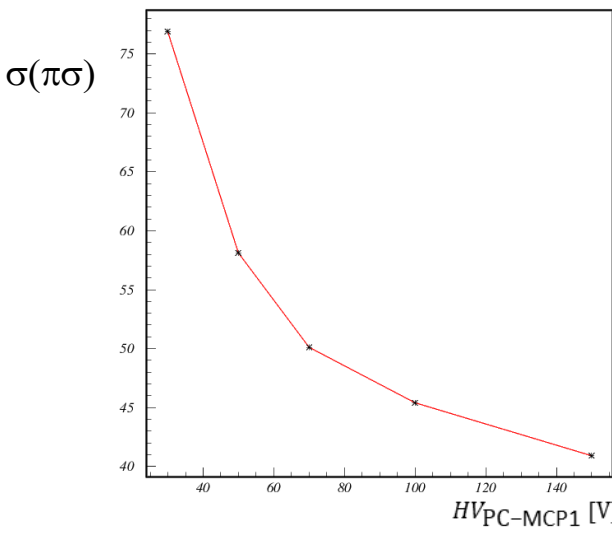
$$d_0 \approx 2l \sqrt{\frac{E_0}{Ue_0}} \sin(\alpha)$$

- and maximal travel time (sideway start)

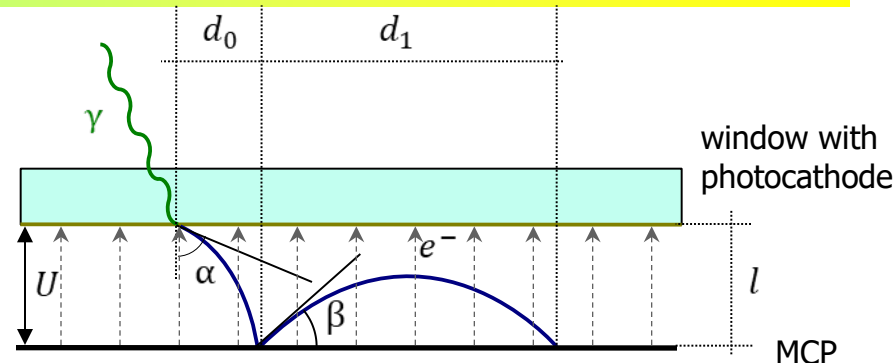
$$t_0 \approx l \sqrt{\frac{2m_e}{Ue_0}}$$

- time difference between downward and sideways initial direction

$$\Delta t \approx t_0 \sqrt{\frac{E_0}{Ue_0}}$$



Time resolution vs PC-MCP1 voltage



Backscattering delay and range (maximum for elastic scattering):

- maximum range vs. angle

$$d_1 = 2l \sin(2\beta)$$

maximum range for backscattered photoelectron is twice the photocathode – first electrode distance

- maximum delay vs. angle

$$t_1 = 2t_0 \sin(\beta)$$

maximum delay is twice the photoelectron travel time

- time of arrival of elastically scattered photoelectrons: flat distribution up to max  $t_1 = 2t_0$

Example ( $U = 200 \text{ V}$ ,  $E_0 = 1 \text{ eV}$ ,  $l = 6 \text{ mm}$ )

photoelectron:

- max range  $d_0 \approx 0.8 \text{ mm}$
- p.e. transit time  $t_0 \approx 1.4 \text{ ns}$
- $\Delta t \approx 100 \text{ ps}$

backscattering:

- max range  $d_1 = 2l = 12 \text{ mm}$
- max delay  $t_1 = 2.8 \text{ ns}$

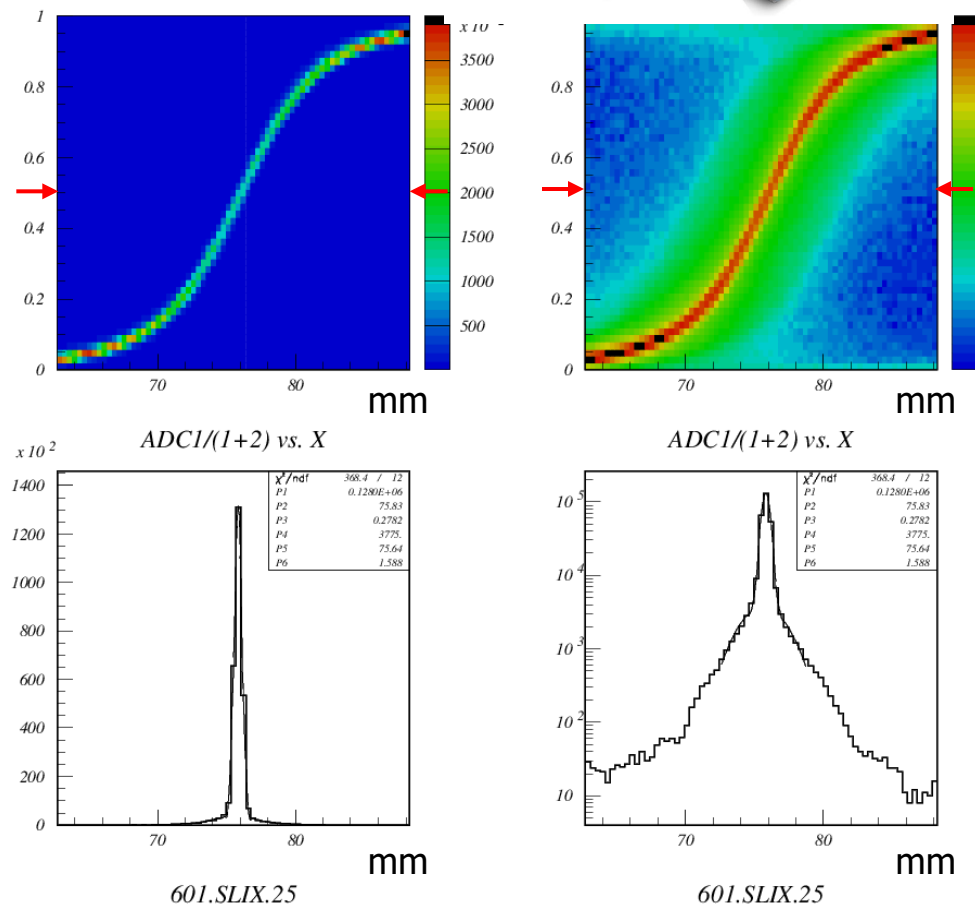
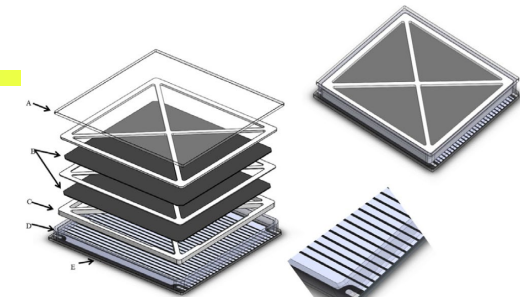
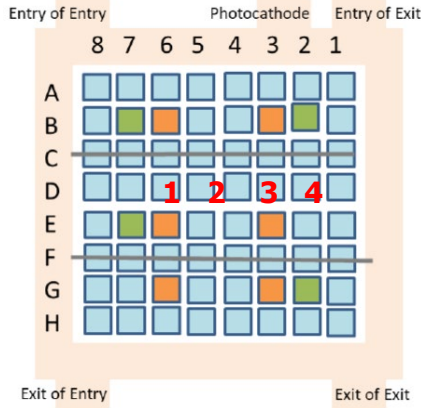
S.Korpar@PD07

# LAPPD – charge sharing in Gen II capacitively coupled electrode readout

- fraction of the signal on channel 3 vs laser spot

x position:  $f(x) = \frac{q_3}{\sum_i q_i}$

- scan between the centres of pads 2 and 3 (top)



- central slice where signal is equally split between the pads (bottom)
- narrow peak is due to the light spot size and photoelectron spread
- longer tail from photoelectron backscattering -  $\approx 6$  mm on each side  $\rightarrow \approx 3$  mm PC – MCP1 distance

# Whole-body scanner simulations

Simulation: GATE v8.1

Geometry:

- Based on Siemens Biograph Vision PET/CT
  - ring: 19 modules (Axial FOV: 26.3 cm)
  - module: 2 x 8 block detectors
  - block detector: 4 x 2 mini-blocks
  - mini-block: 5 x 5 crystal array
  - crystal:  $3.2 \times 3.2 \times 20 \text{ mm}^3$

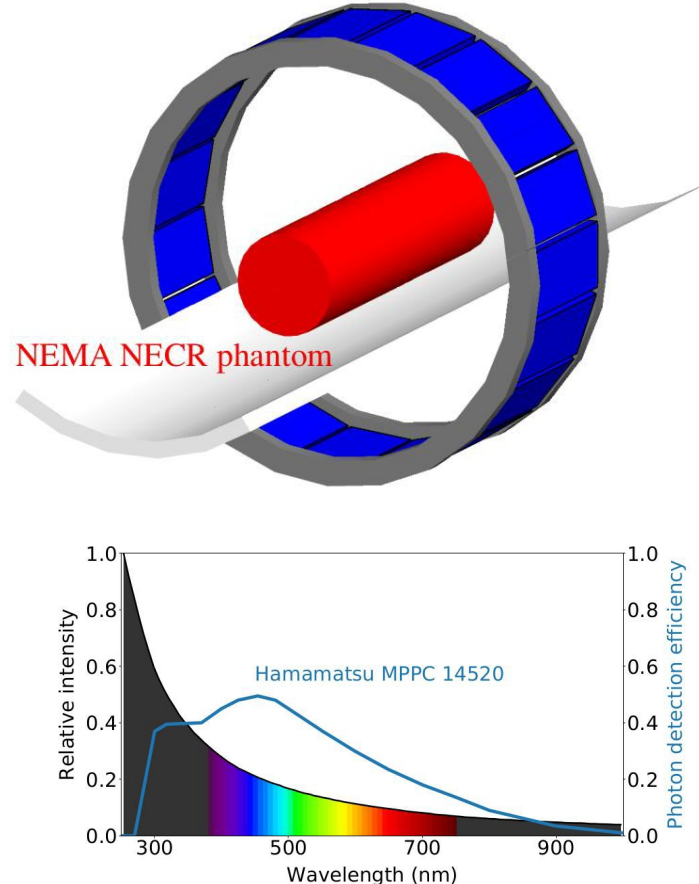
Optical simulations (Cherenkov):

- Surfaces: Geant4 UNIFIED model
  - reflector (diffuse,  $R=95\%$ ,  $n=1.0$ )
  - black ( $R=0\%$ ,  $n=1.5$ )
- Photodetector: Hamamatsu S14520 SiPM
  - Single Photon Time Resolution (SPTR): 70 ps FWHM
  - SiPM dark counts not modeled

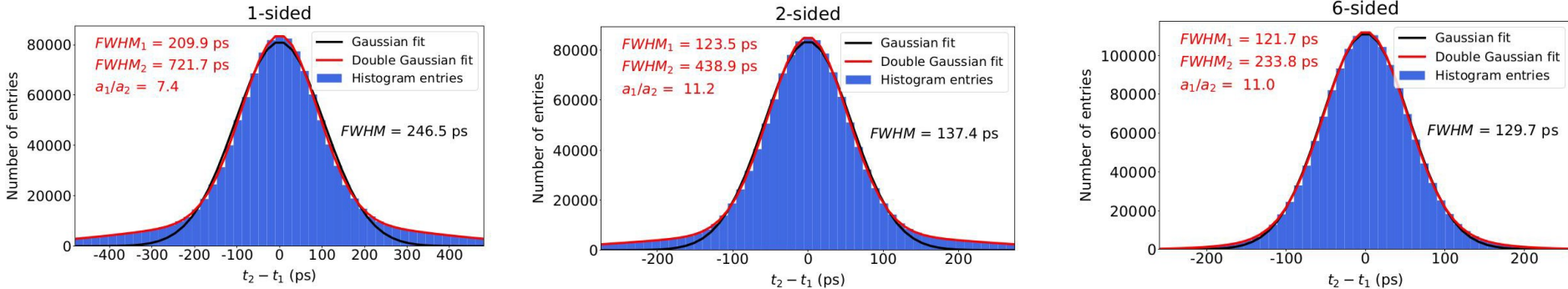
Reconstruction: CASToR v3.1.1

Custom double Gaussian TOF kernel

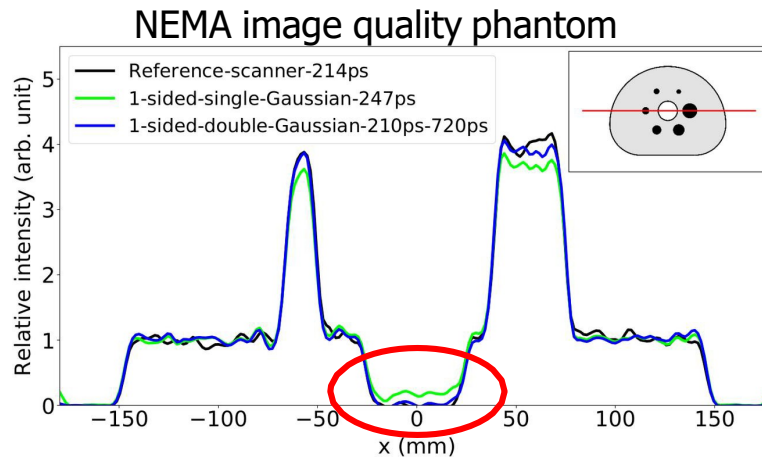
OSEM-8it:5sub, 1.6 mm voxel, 5 mm filter



# Results: CTR distributions



TOF kernel:  
-single Gaussian  
-double Gaussian

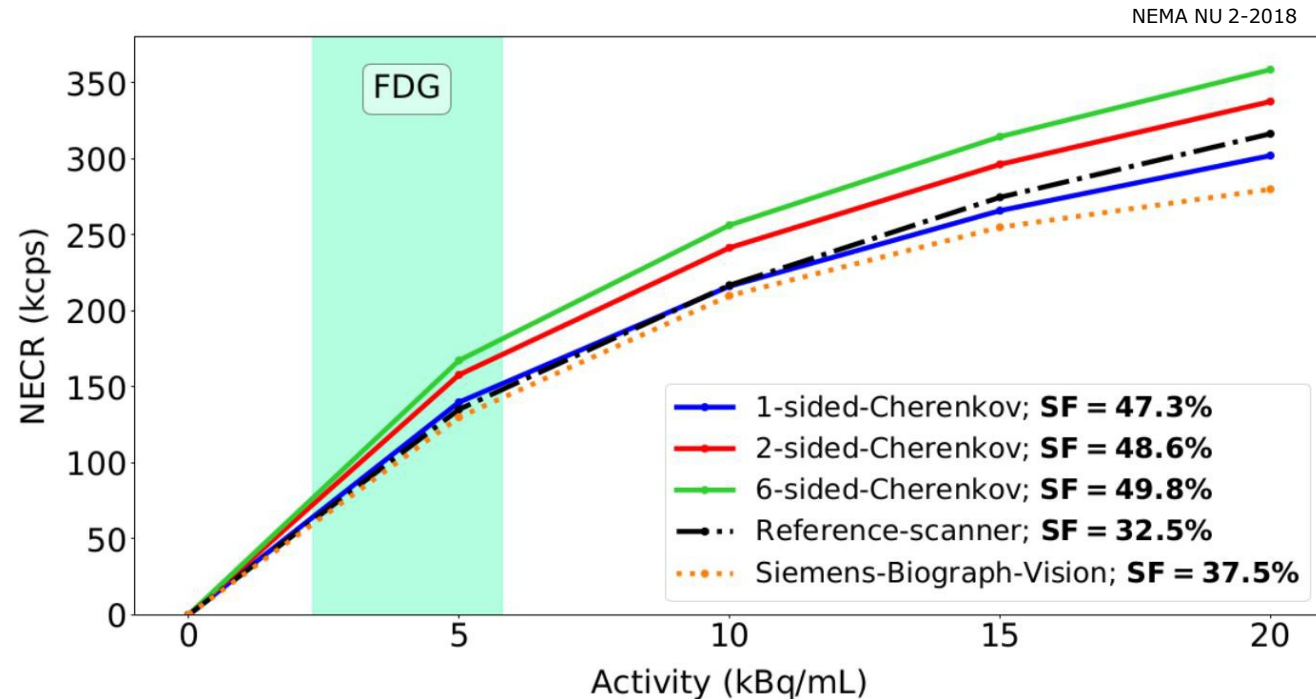


G. Razdevšek *et al.*, IEEE TRPMS 7 (2023) 52

# Results: NECR - Noise Equivalent Count Rate

- Noise Equivalent Count Rate\*:  $NECR = \frac{true^2}{true + random + scatter}$ 
  - not influenced by TOF
- Scatter Fraction:  $SF = \frac{scatter}{true + scatter}$

G. Razdevšek *et al.*, IEEE TRPMS 7 (2023) 52



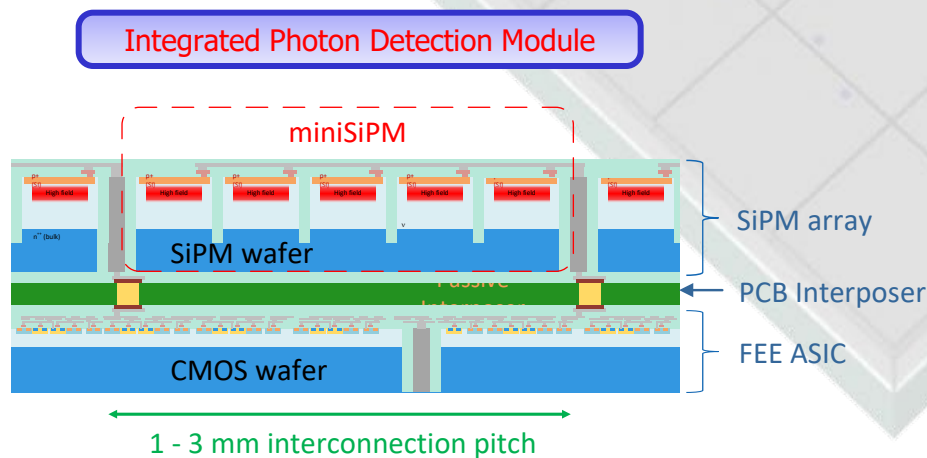
\*The “Noise Equivalent Count” is the number of counts from a Poisson distribution (standard deviation estimated by  $SQRT\{N\}$ ) that will yield the same noise level as in the data at hand.

# FBK SiPM sensor

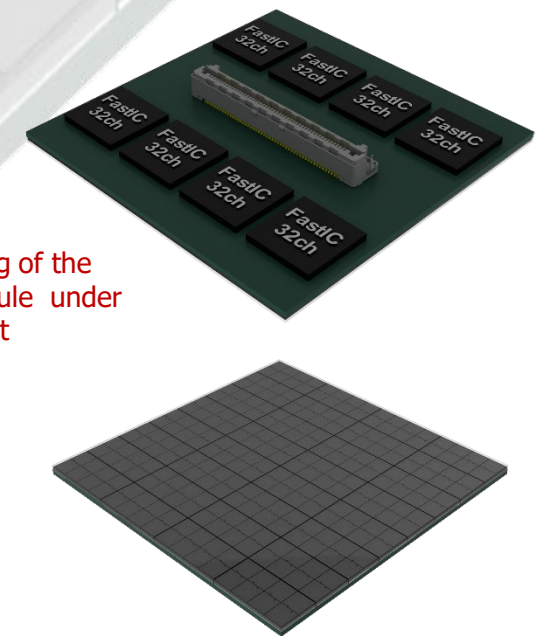
## 2.5D integrated SiPM tile for improved timing

In the short and medium term - medium density interconnection

- excellent timing on large photosensitive areas w/o increasing complexity + cost too much.
- SiPMs with TSVs down to 1 mm pitch are connected to the readout ASIC on the opposite side of a passive interposer, in a 2.5D integration scheme.



Conceptual drawing of the photon detector module under development



Hybrid SiPM module being developed for ultimate timing performance in TOF-PET